CHALMERS

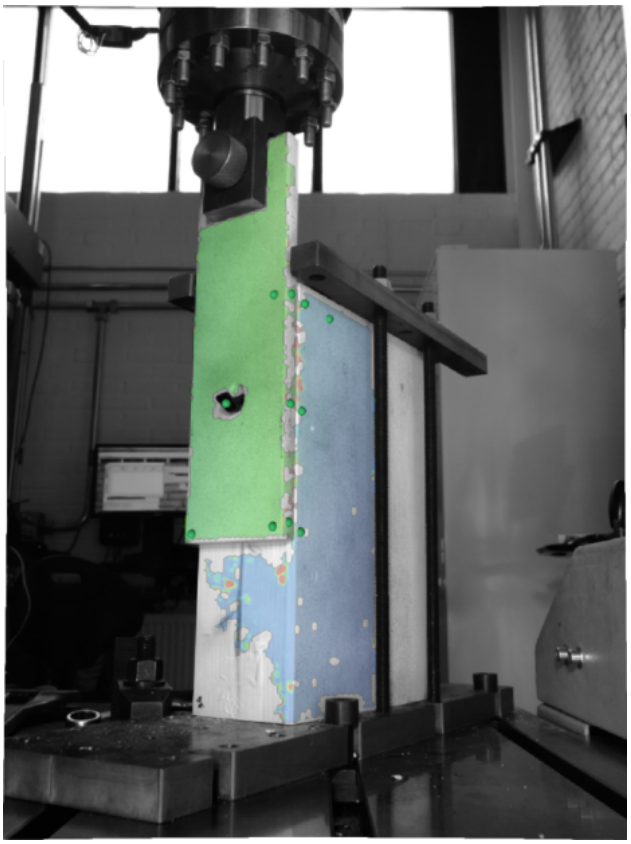

Experimental investigation of steel-to-timber joints with inclined self-tapping screws

A parametric study evaluating load-displacement behavior and testing configurations in quasi-static testing

Bachelors's thesis in Civil Engineering

OLLE DAHLBERG & NICKLAS VALLSTRÖM

DEPARTMENT OF STRUCTURAL ENGINEERING
CHALMERS UNIVERSITY OF TECHNOLOGY
Gothenburg, Sweden 2024
www.chalmers.se

Bachelors's thesis 2024

Experimental investigation of steel-to-timber joints with inclined self-tapping screws

A parametric study evaluating load-displacement behavior and testing configurations in quasi-static testing

Bachelor's thesis in Civil Engineering

OLLE DAHLBERG & NICKLAS VALLSTRÖM

CHALMERS

Department of Architecture and Civil Engineering
Structural Engineering
Lightweight Structures
Chalmers University of Technology
Gothenburg, Sweden 2024

Experimental investigation of steel-to-timber joints with inclined self-tapping screws
A parametric study evaluating load-displacement behavior and testing configurations in quasi-static testing
OLLE DAHLBERG & NICKLAS VALLSTRÖM

Supervisor: Dorotea Caprio, Division of Structural Engineering
Examiner: Robert Jockwer, Division of Structural Engineering

Bachelor's thesis 2024
Department of Architecture and Civil Engineering
Division of Structural Engineering
Lightweight Structures
Chalmers University of Technology
SE-412 96 Gothenburg
Telephone +46 31 772 1000

Cover: Visualization of displacement data captured during testing through digital image correlation.

Typeset in LaTeX
Printed by Chalmers Reproservice
Gothenburg, Sweden 2024

Experimental investigation of steel-to-timber joints with inclined self-tapping screws
A parametric study evaluating load-displacement behavior and testing configurations in quasi-static testing

OLLE DAHLBERG & NICKLAS VALLSTRÖM
Department of Architecture & Civil Engineering
Chalmers University of Technology

Abstract

This bachelors thesis addresses the use of inclined self-tapping screws in steel-to-timber joint configurations, exploring their design and load-displacement behavior through both experimental testing and a literature review. The literature review provides an understanding of the design and behavior of steel-to-timber joints, particularly focusing on inclined screws and their governing parameters, stiffness, and load-bearing capacity. Previous investigations within the research area are discussed, highlighting testing configurations and derived analytical equations.

The experimental phase involved the preparation of steel and timber members to assemble the required number of specimens, with the steel plates machined to accommodate different parametric configurations. The tests were carried out using a servohydraulic load frame while collecting load and displacement data through Digital Image Correlation (DIC) and Linear Variable Differential Transformer (LVDT) technology.Results from the experiments illustrated by graphs depicting representative load-displacement behavior of selected parametric configurations highlight that screw inclination, length, pre-tensioning moment, and friction conditions significantly affect joint performance. Specifically, screws inclined at 45-degrees with lengths of 200 and 400mm appear to exhibit the highest load-bearing capacity and elastic stiffness of the testing series. The comparison between asymmetrical and symmetrical configurations revealed that the asymmetrical configuration is a feasible method to test joint behavior, as it produced similar load-displacement curve characteristics.

This study aims to provide information on the application of inclined self-tapping screws in steel-to-timber joints, offering insights into experimental configurations and procedures and into the main parameters of influence.

Keywords: steel-to-timber joints, self-tapping screws, inclined screws, experimental investigation, load deformation behavior, stiffness, load-carrying capacity, ductility, Eurocode 5 (EC5), Digital Image Correlation (DIC)

Experimentell undersökning av stål/trä-förband med lutande självgängande träskruv
En parametrisk studie som utväderar last/deformations-beteende och testkonfigurationer i kvasi-statisk testning
OLLE DAHLBERG & NICKLAS VALLSTRÖM
Department of Architecture & Civil Engineering
Chalmers University of Technology

Sammanfattning

Detta examensarbete undersöker användningen av lutande självgängande träskruvar i stål/trä-förband och behandlar deras design samt last-deformationsbeteende genom en experimentell undersökning och en litteraturstudie.Litteraturstudien ger en förståelse för dimensioneringen och beteendet hos stål/trä-förband med ett särskilt fokus på lutande skruvar och deras huvudsakliga parametrar som styvhet och bärförmåga. Tidigare undersökningar inom forskningsområdet behandlas där testkonfigurationer och härledda analytiska ekvationer belyses.

Den experimentella undersökningen bestod av förberedelser och montage av provkropparna, detta inkluderade infästning av de element provkroppen bestod av - stålplatta, träskruv och limträ. Testerna genomfördes med hjälp av en servohydraulisk lastram, medan last- och deformationsdata samlades in genom Digital Image Correlation (DIC) och Linear Variable Differential Transformer (LVDT)-teknologi. Resultaten från utförda experimentella försök, illustrerade genom grafer som visar representativt last-deformationsbeteende för valda parametriska konfigurationer, visade att skruvlutning, längd, förspänningsmoment och friktionsförhållanden påverkar förbandens beteende. Specifikt visade sig skruvar med 45 graders lutning med längder på 200 och 400 mm uppvisa högst bärförmåga och styvhet i testserien. Jämförelsen mellan den asymmetriska och symmetriska konfiguration visade att den asymmetriska konfigurationen är en passande metod för att testa förbandens beteende, detta då liknande last-deformationsbeteenden kunde bevittnas som den mer vanligt förekommande symmetriska konfigurationen.

Detta examensarbete syftar till att ge information om användningen av lutande självgängade träskruvar i stål/trä-förband, och erbjuda insikter i experimentella konfigurationer och procedurer. Framtida arbete kan använda dessa insikter för att förbättra förståelse och dimensionering genom fortsatta experimentella undersökningar och teoretiska analyser, med fokus på nyckelparametrar och undersökning av variabiliteten hos stål/trä-förband med lutande självgängande skruvar.

Nyckelord: Stål/trä-förband, självgängande skruv, lutande skruv, experimentell utredning, last-deformations beteende, styvhet, bärförmåga, duktilitet, Eurocode 5 (EC5), Digital Image Correlation (DIC)

Acknowledgements

This project took place between January and May 2024, with experimental investigations conducted from January to April. It is part of an ongoing research initiative by the Department of Civil Engineering and Architecture at Chalmers University of Technology. The project was supervised by Dorotea Caprio and examined by Robert Jockwer.

We extend our heartfelt appreciation to Dorotea Caprio for her invaluable supervision and guidance throughout the thesis process and for her assistance in the experimental procedure and data analysis. We also acknowledge Robert Jockwer for his support and encouragement. Special thanks to Sebastian Almfeldt for his supervision in the laboratory and for designing and manufacturing the necessary testing equipment.

Olle Dahlberg & Nicklas Vallström, Gothenburg, May 2024

List of Acronyms

Below is the list of acronyms that have been used throughout this thesis listed in alphabetical order:

ASY	Asymmetric
CLT	Cross Laminated Timber
DIC	Digital Image Correlation
DOP	Declaration of Performance
EC5	Eurocode 5
ETA	European Technical Assessment
EWP	Engineered Wood Product
FEA	Finite Element Analysis
GiR	Glued in Rods
GL	Glue Laminated
GLT	Glue Laminated Timber
HTO	Head Tear Off Failure
LVDT	Linear Variable Differential Transformer
LVL	Laminated Veneer Lumber
SLS	Serviceability Limit State
STS	Self-Tapping Screw
SYM	Symmetric
ULS	Ultimate Limit State
WITH	Withdrawal Failure
WSH	Washer

Nomenclature

Below is the nomenclature of the parameters, constants, and variables that have been used throughout this thesis.

Roman upper case letters

E_{steel}	Modulus of elasticity steel
F_{ax}	Anchorage capacity
$F_{ax,Ed}$	Design axial stress
$F_{ax,Rd}$	Design axial strength
$F_{ax,Rk}$	Characteristic anchorage capacity
$F_{V,Rk}$	Single shear capacity
$F_{v,Ed}$	Design shear stress
$F_{v,Rd}$	Design axial stress
$K_{\parallel}$	Stiffness parallel to grain
$K_{\perp}$	Stiffness perpendicular to grain
K_{ser}	Stiffness in serviceability limit state
K_{SLS}	Stiffness in serviceability limit state
$K_{SLS,ax}$	Axial stiffness in serviceability limit state
$K_{SLS,v}$	Shear stiffness in serviceability limit state
K_u	Stiffness in ultimate limit state
M_{tors}	Torsional moment of pre-tensioning
M_y	Yield moment of dowel
$M_{y,k}$	Characteristic yield moment of fastener
$M_{y,Rk}$	Yield moment of fastener
R_0	Parallel resilience
R_{90}	Perpendicular resilience
R_{ax}	Axial resilience

R_v	Shear resilience

Roman lower case letters

d	Core screw diameter
d_{core}	Inner core diameter of fastener
d_{ef}	Effective diameter of fastener
f_h	Embedment strength of timber
$f_{h,0,k}$	Characteristic embedment strength parallel to fiber direction
$f_{h,\alpha,k}$	Characteristic embedment strength under load directed in an angle α to the grain direction
$f_{h,k}$	Characteristic embedment strength of timber
$f_{tens,k}$	Characteristic tensile capacity of fastener
$f_{tens,k}$	Characteristic torsional capacity of fastener
f_u	Tensile strength of fastener
$f_{v,roll}$	Rolling shear
l_{ef}	Effective length embedded in wood
l_w	Length threaded part embedded in wood
m_{dtr}	Mass of oven-dried wood
m_u	Mass of moist wood
t_1	Thickness of timber member
u	Moisture content of wood
x_1	Reduced embedment length

Greek letters

α	Angle between fastener axis and grain direction
ϵ	Load to grain angle or inclination of fastener
κ_{90}	Correction factor for material type
κ_d	Correction factor
μ	Coefficient of friction
ρ_{12}	Density of wood at 12% moisture content
ρ_k	Characteristic density of wood

Contents

List of Figures

List of Tables

1
Introduction

1.1 Background

Timber has been appreciated throughout human history for its abundance, ease of transformation, and mechanical properties [6]. Man-made wooden structures have evolved from simple shelters crafted by early human civilizations to towering wooden skyscrapers created by contemporary architects and engineers. This increase in scale and complexity demands increased knowledge about the structural behavior of timber structures to facilitate future design and improve reliability.

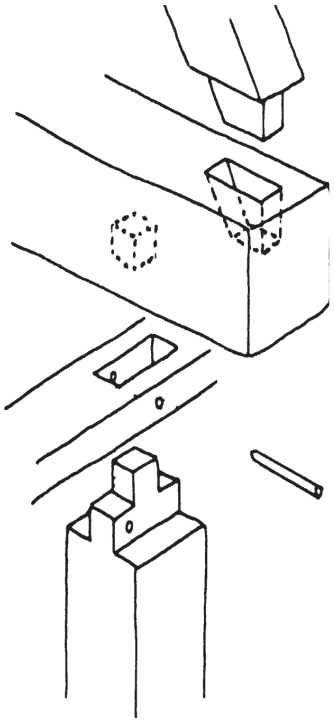

Figure 1.1: Example of traditional Japanese joinery. [1]. Reprinted with permission.

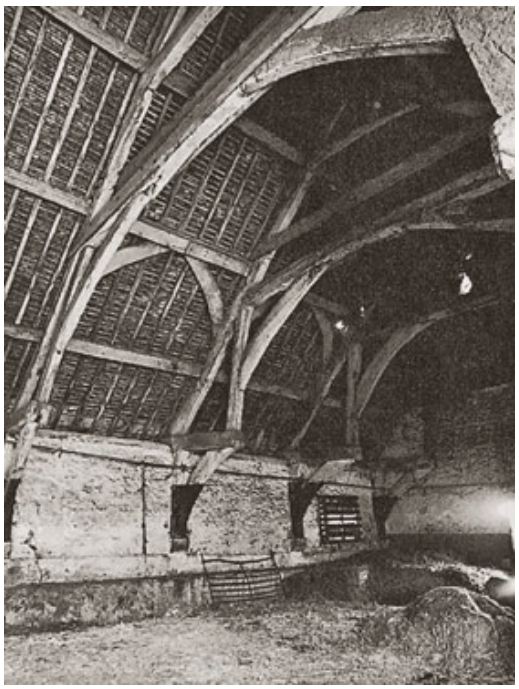

Figure 1.2: English barn structure with traditional joinery. [1]. Reprinted with permission.

Despite the long-standing utility of timber as a construction material, fears that fires would spread uncontrollably in developing urban societies led to building codes that would limit the scale of timber construction, causing society to overlook the high performance capabilities of timber for centuries [6]. However, the increasing need for more sustainable construction and the creation of new engineered wood

products has sparked a new interest in timber structures [7]. As a result, large-span structures and high timber buildings are being built around the world[8]. The load capacity, stiffness, and ductility of a structure are heavily dependent on the characteristics of the joints within the structural system [10]. The integration of steel components into timber joinery represents a leap forward in addressing the limitations of traditional techniques, illustrated in Figures 1.1 and 1.2. Steel-to-timber joints offer numerous benefits, including increased load carrying capacity and ductility, coupled with greater design flexibility [11]. The increased adoption of self-tapping screws in timber joint design in recent years is due to multiple reasons. Ease of assembly, high load capacity and stiffness, as well as providing multi-directional load transfer into the timber [11], [12]. Figure 1.3 illustrates a modern steel-to-timber joint with inclined self-tapping screws.

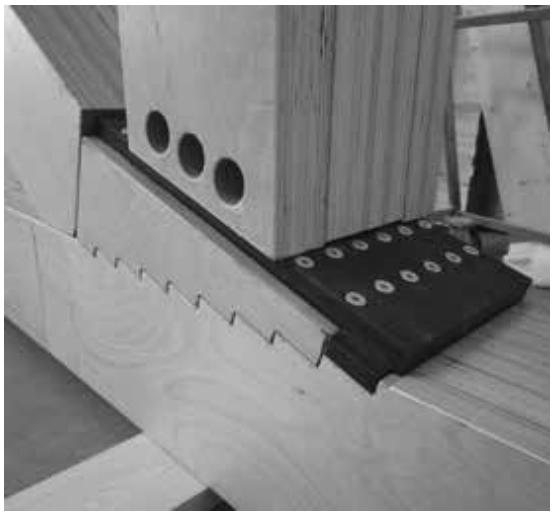

Figure 1.3: Extended multiple step steel-to-timber joint with self-tapping screws. [9]. Reprinted with permission.

Methods for defining structural reliability have been developed to aid in the design and structural analysis of structures by adapting them to building codes and regulations. According to Köhler [13], considerable effort and progress have been made to increase consistency in assessing safety in steel and concrete structures.

However, the development of the structural design code for timber has been hindered by the complexity of the material and by a more empirical and less scientific approach. The calculation of the load-carrying capacity is covered in the current generation of design code, Eurocode 5 [14] through the European yield model developed by Johansen [15] (developed in 1949). The mechanical behavior of joints is also described through elastic stiffness and ductility. For this reason, experimental testing plays a key role in evaluating the performance of materials and joints under various loading conditions, providing empirical data to inform and modernize design standards and guidelines [16].

This thesis aims to aid these developments by conducting a parametric experimental campaign on steel-to-timber joints with inclined self-tapping screws to evaluate different testing configurations, load-displacement behavior with regard to load-bearing capacity, stiffness, ductility, and failure modes. The results can come to inform future experimental investigations, provide empirical data to support the development of analytical models, and potentially suggest improvements in joint design.

1.2 Aim

The aim of the thesis is to gain a deeper understanding of the load-displacement behavior of timber joints with inclined self-tapping screws (STS). This will be done through a literature review as well as experimental efforts that will investigate the parameters of influence including: load-to-screw axis angle, length of screw, pre-tensioning force, and the friction type in the steel-to-timber joints.

The experimental campaign included a series of parametric tests with the purpose of answering the following research questions:

- What are the main factors and how do they influence the shape of the load-displacement curves of the joint in question?
- Is it feasible to test this type of joint in an asymmetric test setup configuration?

1.3 Methodology

1.3.1 Literature review

In the initial phase of this study, a literature review was conducted to improve understanding of timber joints with inclined self-tapping screws. The review included a review of relevant academic articles, books and industry standards to gather information on material properties, structural behavior, and design principles of the relevant joints.

1.3.2 Experimental campaign

Specimen preparation

Timber specimens were prepared from GL30c glue-laminated timber beams. Steel plates and self-tapping screws were selected on the basis of their material properties and dimensions to ensure compatibility and performance under testing conditions. Each specimen was assembled with an attention to uniformity and consistency to minimize variability due to differences in assembly.

Test set-up

The experimental setup involved testing rigs for the fixing of the specimens, manufactured at Chalmers University Structures Lab, mounted in a servo-hydraulic load frame. This testing machine is capable of running displacement-controlled quasi-static tests, allowing for simultaneous measurement of displacement and load responses. This setup ensured that the tests could be accurately controlled and repeated under safe and consistent conditions.

Data collection and Analysis

DIC coupled with applied load data from the load cell of the testing rig served as the primary data collection method in the initial study. The results of the DIC data, analyzed using the GOM Correlate 2018 software, were plotted in MATLAB to illustrate the load-displacement behavior. DIC was used in the study to gain a better understanding of the test set-up.

1.4 Limitations

The following section discusses the limitations of the study. Although the research provides insight into the behavior of steel-to-timber joints using self-tapping screws, there are some factors that limit the findings. Keeping these limitations in mind is important to interpret the results correctly and also to suggest areas for future research.

Constraints in Planning and Preparation of Experimental Campaign
Planning and preparation of the experimental campaign were limited by the available time frame and the knowledge base of the authors. As a result, aspects of the experimental campaign and methodology were not part of the thesis project.

Limitations in Calculations for Input Values and Failure Modes
Calculations used to determine input values and predict failure modes are subject to limitations. The authors of this thesis did not perform these calculations.

Literature Review and Design Methodologies
The literature review and design methodologies predominantly center on timber joints with inclined screws with associated parameters and failure modes. While this provides a understanding within this specific domain, it may overlook insights and methodologies relevant to other joint types or materials.

Limited Analysis on Test Data
The analysis conducted on the test data is limited. Although efforts were made to analyze the data rigorously, constraints such as time and resources may have restricted the depth and breadth of the analysis. Consequently, certain insights or correlations within the data may not have been fully explored.

Restriction of Parameters
Parameters considered in the study focus primarily on angle, pretensioning moment, length of screw, and friction. However, there are other parameters, such as material properties, joint configurations, and environmental conditions, which could also influence the load-displacement curves.

Recognizing these limitations is important when considering the findings of this thesis and understanding their implications within the research area of timber construction and joint design.

1.5 Outline

Chapters 1 through 4 introduce the thesis, covering background, aim, methodology, material properties, and a literature review focused on timber joint design and behavior as well as timber joints with inclined self-tapping screws. Chapters 5 and 6 guide the reader through the experimental campaign and its results and accompanying discussion. Chapter 7 ends the thesis with a conclusion and recommendations for future research in the field, as well as an credits section.

Chapters 1 provide the reader with background as well as the aim, methodology, and limitations of the thesis.

Chapter 2 describes physical properties of the included materials of the test specimen.

Chapter 3 includes general information about the behaviour and design of dowelled-type timber joints.

Chapter 4 is a description of previous investigations in the field of timber joints with inclined self-tapping screws.

Chapter 5 details the experimental campaign, providing an overview of the preparations, test setup, and data collection procedures.

Chapter 6 illustrates the main findings in the experimental campaign as well as discusses the results and overall testing procedure.

Chapter 7 presents the reader with a conclusion as well as suggestions for future work and credits.

2
Material properties

The test specimens used during the experimental testing phase generally include one glue laminated timber member, one or two machined steel plates, and self-tapping steel screws to create the joint. Familiarity and basic knowledge of the properties and behavior of timber and steel are of importance in understanding the theoretical discussions addressed in subsequent chapters. Although prior understanding of these materials is assumed, the following chapter provides a selection of basic knowledge regarding these materials.

2.1 Timber

2.1.1 Overview

Timber as a structural material shows a wide variety when considering properties that influence structural behavior, e.g. moisture content, density, and temperature. Wood exhibits varying properties in different orientations. This anisotropy is due to the fact that wood is a natural material with an elongated cellular structure. [2].

2.1.2 Wood physics

A main factor that influences the properties of wood is water and changes in moisture content. Because wood is a hygroscopic material, the moisture content in wood is dependent on the humidity in the surrounding air. It can rise due to contact with free water by capillary forces but also by adsorption of water vapour from surrounding air [3].

When below the fiber saturation point, around 28%, the moisture content has a large influence on fundamental characteristics, e.g., strength and stiffness, deformation, thermal properties and durability. The decline in strength is governed by the molecular binding forces within the wood, and the ingress of water will force the cellulose chains apart. Dry wood generates a proximity in the cellulose chains that generates strong intermolecular forces; hence, the presence of water weakens the cell walls. To further highlight the impact of moisture content, a one percent increase in wood moisture content results in a six percent decrease in compressive strength parallel to the grain.

This reinforces the fact that moisture must be considered in the design process and by structural engineers. The established definition of moisture content (2.1) is the ratio of the mass of water to the mass of dry wood [2].

$$u = \frac{m_u - m_{dtr}}{m_{dtr}} \cdot 100 \qquad [\%] \tag{2.1}$$

where

u	Moisture content of wood
m_u	Mass of moist wood
m_{dtr}	Mass of oven-dry wood

Another parameter influencing the properties of wood is the ratio between its mass and volume, known as its density. Positive correlations can be seen from a higher density, e.g. higher strength and lower deformations. Local ambient conditions such as climate, soil, and exposure to sunlight have a correlation with density. This affects the proportion of the so-called latewood and earlywood in the timber, where latewood has a higher density due to thinner cell walls and a larger cell lumen [2].

Moisture content also has an effect on density, as both the mass and volume are moisture dependent. Density is therefore sometimes defined as in relation to moisture content, where a commonly used definition in timber engineering is the density at 12% moisture content, ρ_{12}. When used in standard timber strength tests, ρ_{12} is the moisture content used [3]

2.1.3 Mechanical properties

Natural timber characteristics such as knots, spiral grain angle, reaction wood and juvenile wood affect the behavior of timber specimens. These anomalies, such as knots, can induce large local stresses compared to a clear wood specimen. When a clear wood specimen is tested, independently of anomalies, a clear anisotropic behavior is noticed. This behavior originates from the wood structure and the tubed shaped cell in a lignin matrix i.e. grain directions [3].

When loaded in different grain directions, the wood shows different mechanical behavior. In a pure tension test loaded parallel to the grain direction, an almost linear stress-strain relationship is observed. With this test set-up, a strength of 100 MPa can be achieved, although a brittle failure is expected (2.1). In contrast, if the wood is loaded perpendicular to the grain direction in tension, less load is required to break or pull the fibers apart. The expected failure load around 0,5 MPa is anticipated in this load direction (2.2).

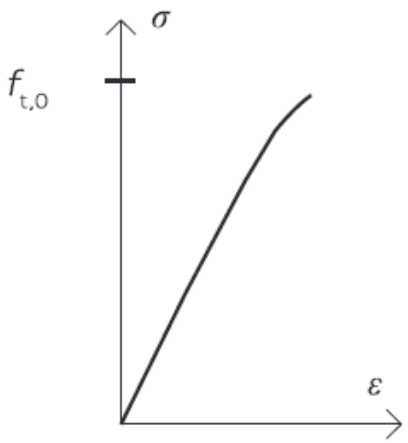

Figure 2.1: Stress-strain relationship for clear wood loaded in tension parallel to fibre direction.[3]. Reprinted with permission.

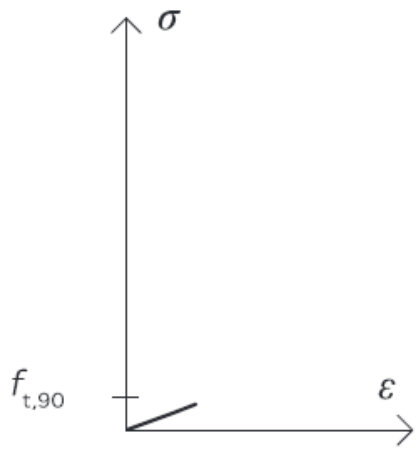

Figure 2.2: Stress-strain relationship for clear wood loaded in tension perpendicular to fibre direction.[3]. Reprinted with permission.

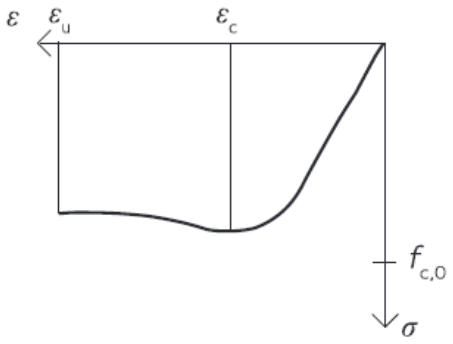

Figure 2.3: Stress-strain relationship for clear wood loaded in compression parallel to fibre direction.[3]. Reprinted with permission.

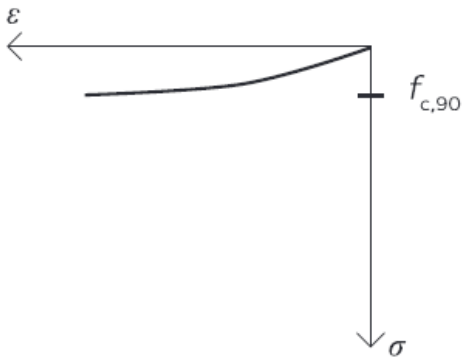

Figure 2.4: Stress-strain relationship for clear wood loaded in compression perpendicular to fibre direction.[3]. Reprinted with permission.

The parallel compression forces that act on the wood will cause a different behavior than those in tension. Due to the orientation of the fibers, an axial compression load will cause a more stable stress-strain behavior, with the possibility of withstanding large loads around 80 MPa. The failure mode of such a test setup will cause buckling in the fibers as a result of plasticity in the material, as shown in Figure 2.3.

The last mode, compression perpendicular to the grain direction, will cause crushing in the tube-shaped wood cells. This occurs under low forces; consequently, the strength in this direction is around 3-5 MPa, as shown in Figure 2.4 [3].

As mentioned above, sawn timber contains anomalies that can cause large local stresses compared to clear wood specimens. Using a standardized methodology according to the European Standard SS-EN 384 [17] and SS-EN 408 [18], the characteristic values of strength and stiffness can be evaluated [3].

2.2 Steel

Steel is widely used in modern construction because of its structural properties such as strength and ductility, as well as specific practical advantages such as versatility and cost-effectiveness. In this section, a brief overview is provided on the composition and properties of steel, within a construction material context, focusing on key characteristics and some theoretical background that will provide context for the work on steel-to-timber joints in this thesis.

2.2.1 Composition

Steel is an alloy primarily composed of iron with carbon and various other elements incorporated to meet specific performance needs and applications. As in other technical metals the atomic structure of steel is poly crystalline, where its smallest component, the unit cell, forms grains in a crystal lattice formation. This crystal lattice form plays a crucial role in determining the properties and mechanical behavior of steel [4].

2.2.2 Mechanical properties

While wood exhibits anisotropic mechanical properties, steel used in construction is generally regarded as isotropic, meaning that its mechanical properties are consistent regardless of the direction of load. This lack of a weak direction in the material makes it a highly appropriate building material and greatly simplifies the structural analysis related to deformation and failure. This behavior is illustrated in the four stress-strain relationships plotted in Figure 2.5 showing the capacity of steels to sustain elastic and plastic deformations.

[4] states that during the elastic deformation phase, the stress-strain curve remains linear, indicating a direct proportionality between stress and strain. This linear relationship is due to the reversible displacement of atoms within the steel crystal lattice. As the load increases, the atoms are displaced further, yet upon unloading within this elastic region, the material returns to its original configuration without any permanent deformation, as the lattice structure remains unchanged. To achieve small deflections and no lasting deformations to your structure in the serviceability limit state, you therefore want to design your structure to permanently remain in the elastic region.

At a certain load level the graph diverges to a more or less horizontal state with non-increasing load and increased deformation [4]. This point of change is known as the yield point of the material. This behavior is due to the fact that steel has inherent defects in the crystal lattice structure called dislocations, where essentially there are missing atoms within the lattice.

[4] also states that with continued loading, movements of dislocations will result in plastic deformation. This plastic behavior is the main factor in ductile material when it refers to the ability to undergo permanent deformation under applied stress without fracturing in a brittle way. With continued deformation, the number of dislocations increases and the ability to move and redistribute stresses decreases. This induces deformation hardening which can be observed in the apparent increase in load capacity with increased deformation before failure occurs.

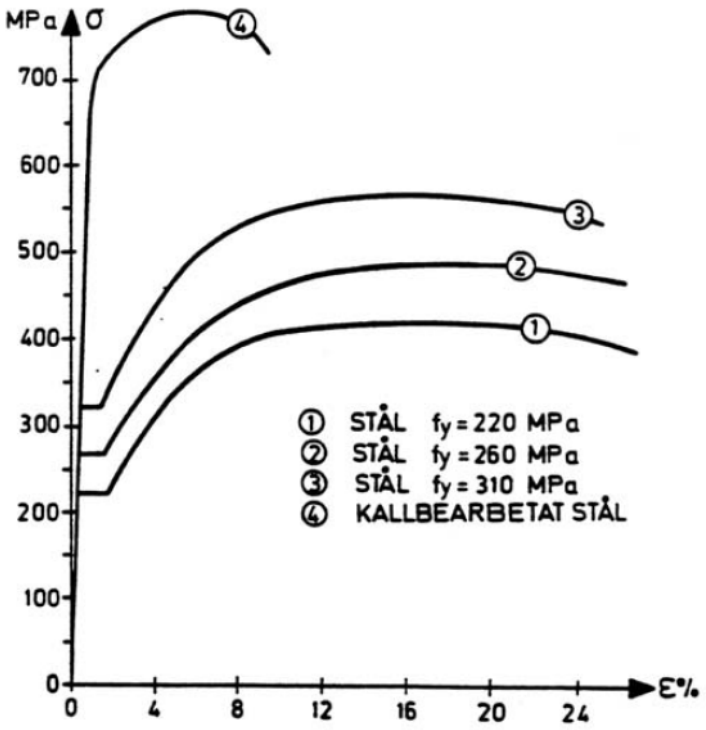

Figure 2.5: Typical stress-strain behaviour of construction steel with varying qualities. [4]. Reprinted with permission.

3

Behavior and Design of dowelled-type timber joints

3.1 Introduction

To assemble timber elements into a structural system, joints are required. These connections will in part govern the structural behavior of the entire system, and the parameters that affect them must be taken into account when designing complex timber structures. Since the joints within the system tend to be weaker than the members that are joined, careful design is therefore an important safety factor [5].

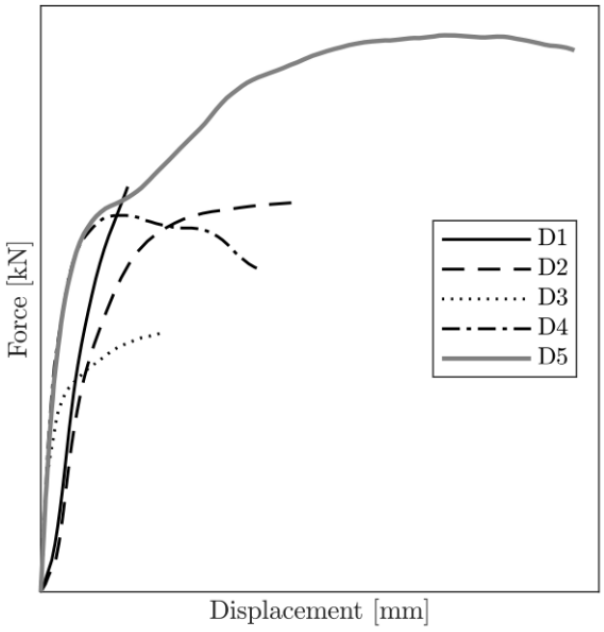

Figure 3.1: Representative load-displacement shapes for dowel-type joints. [19]. Reprinted with permission

Considering the load-displacement curves of timber joints, they exhibit a wide range of shapes, influenced by numerous parameters. Factors such as load-to-grain angle, load-to-fastener angle, load duration, and testing methodology affect these curves. Material parameters, including steel grade, timber species, and density, also play a role, along with geometric parameters such as end and edge distances, fastener spacing and diameter [19].

As depicted in Figure 3.1, timber joints can exhibit various behaviors, such as brittle behavior reminiscent of curve D1, which shows an almost elastic response before sudden failure. Plastic regions, as seen in curve D2 with a plastic plateau, or curve D3 with a hardening branch and unclear load-bearing capacity, can also occur. Curves D4 and D5 represent extensive plastic behavior. Studying Figure 3.1, a non-linear correlation can also be observed [19].

The different kinds of joints in timber structures can be classified into the following categories [5]:

3.1.1 Traditional timber joints

Traditional joining techniques have their origins in the iron age [1] and can be observed in timber structures to this day. These joints are characterized by mortise and tenon joinery with locking wooden dowels. Joints like these are time-consuming to manufacture due to the handmade details and subsequently expensive. Furthermore, limitations in load transfers can be seen in these joints since compression forces is the main transmitted load [5].

3.1.2 Glued joints

Glued joints are used to connect elements but also for reinforcing timber, e.g. perpendicular to the grain direction. Is commonly applicable in controlled environments. Examples of glued joints are Glued in Rods (GiR), and the joining of individual lamellas in GLT and LVL [5].

3.1.3 Dowel-type joints

This is the most common type of joint, including those that employ nails, screws, wooden dowels, bolts, and nail plates. Their versatility, effective load-transfer mechanisms, and low economic costs make them widely used. For increased safety in timber structures, dowelled joints can be designed for ductile behavior [5].

Fully threaded self-tapping screws, a type of dowel fastener, exhibit a stress distribution along the entire threaded axis, resulting in a resistance proportional to the threaded length. These screws also demonstrate high stiffness characteristics [20]. The following section describes the fundamental knowledge behind this type of joints as well as joint design and relevant parameters.

3.2 Parameters

The load carrying capacity of a dowelled-type screw joint is influenced by three main parameters:

Embedment strength of wood, f_h, quantifies the ability of the fastener to remain securely embedded within the wood without experiencing premature failure or withdrawal.
This strength is influenced by factors such as wood species, density, moisture content, and fastener design. The angle between the load and grain direction also has an influence on embedment where the highest strength is obtained parallel to the grain in compression [5].

The yield moment of the dowel, M_y, refers to the maximum moment that can be applied to the dowel before reaching its yield moment and subsequently forming one or more plastic hinges [5]. In the context of dowelled fasteners, which typically involve a pin or dowel inserted through two or more components to join them, the yield moment indicates the point at which the applied torque or bending force causes the fastener material to exceed its elastic limit and enter into plastic deformation.

Anchorage capacity, F_{ax}, of dowelled-type fasteners refers to the maximum load they can support before losing their grip or failing to sufficiently anchor the joined components [5]. This capacity depends on factors such as material properties, joint geometry, and installation method.

In addition to the parameters mentioned above, geometric factors, such as edge and end distances, are involved in the design, which are crucial to prevent splitting and brittle failure. The inner and outer diameters of the fastener threads also play a significant role in the case of stress distribution, as does the penetration depth, which contributes to the load carrying capacity [2]

3.3 Design according to Eurocode 5

The work of Johansen [15] significantly influences the equations for evaluating lateral joint capacity in the current EC5 [14] design code [21]. These equations indicate that the capacity is limited by the point where the embedment strength is achieved in at least one of the connected timber members.

Furthermore, under specific conditions, the simultaneous appearance of plastic hinges in the fastener further constrains this limit. The failure mechanism depends on the geometry of the joint and the properties of the material, with particular emphasis on variables such as the plastic bending moment of the dowel or the embedment strength of the timber or wood-based material as mentioned above [2].

3.3.1 European Yield Model

In steel-to-timber connections using robust steel plates, the steel plate functions as a secure support for the fastener. The holding strength of the steel plate is much higher than that of timber or wood-based materials and is considered infinite according to the Johansen equations. This leads to the formation of plastic hinges within the shear plane between the steel plate and timber when failure modes cause plastic hinges to develop. If the thickness of the steel plate is equal to or greater than the diameter of the fastener, plastic hinges can be expected within the shear plane. The EC5 [14] standard shows potential failures of steel-to-timber joints with thick steel plates and their failure modes, as shown in Figure 3.2 [2].

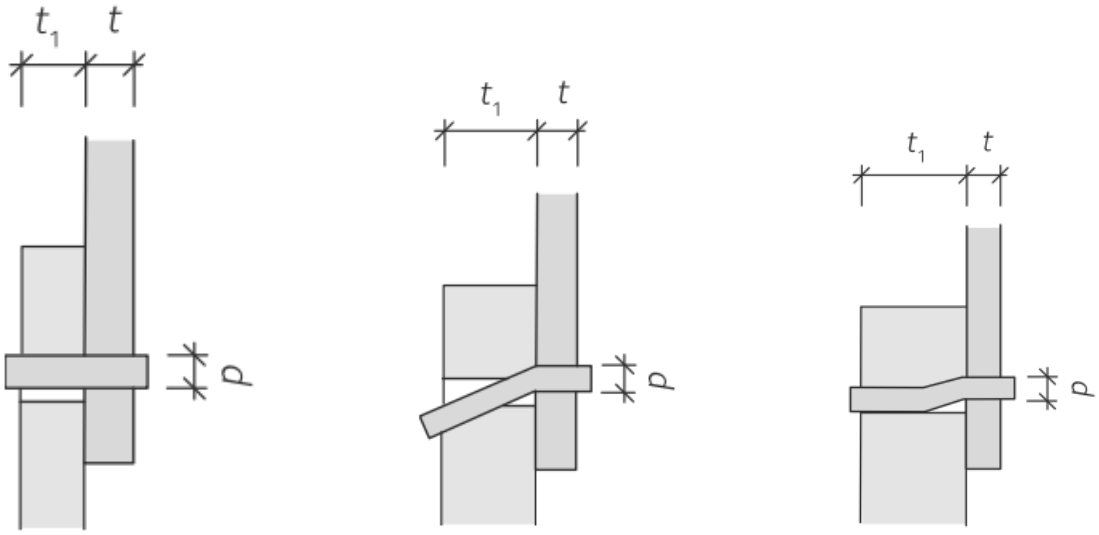

(a) Failure mode **A** **(b)** Failure mode **B** **(c)** Failure mode **C**

Figure 3.2: Various failure modes for steel-to-timber joints [5]. Adapted with permission.

The single shear capacity by failure mode A, as illustrated in Figure 3.2, can be calculated according to Equation 3.1, which is dependent on the embedment strength, the thickness of the timber member, and the diameter of the fastener.

$$F_{v,Rk} = f_{h,k}\, t_1\, d \tag{3.1}$$

Failure mode B as described in 3.2 depends on the embedment strength of the timber, $f_{h,k}$, thickness of the timber member t_1, the diameter of the screw core d and the yielding moment of the fastener $M_{y,Rk}$. An additional strength due to the rope effect caused by the plastic hinge can also be added as the last term.

$$F_{v,RK} = f_{h,k}\, t_1\, d \left(\sqrt{2 + \frac{4\, M_{y,RK}}{f_{h,k}\, d\, t_1^2}} - 1 \right) + \frac{F_{ax,Rk}}{4} \tag{3.2}$$

The single shear capacity according to failure mode C also includes $f_{h,k}$, d, $M_{y,Rk}$ and additional strength due to rope effect:

$$F_{v,Rk} = 2.3\sqrt{M_{y,Rk}\, f_{h,k}\, d} + \frac{F_{ax,Rk}}{4} \tag{3.3}$$

The characteristic embedment strength ($f_{h,k}$) (3.4) for bolts and dowels with all diameters, pre-drilled, when loaded parallel to the grain, is expressed in units of N/mm^2 as [5]:

$$f_{h,k} = 0.082\,(1 - 0.1\,d)\;\rho_k \tag{3.4}$$

Consideration must be given to the impact of the angle between the force and grain directions on embedment strength. Particularly, for larger fastener diameters, there is a decrease in embedment strength as the angle between the force and grain directions increases. In EC5 [14] this is taken into account by applying Hankinson's equation 3.5 [2].

$$f_{h,\alpha,k} = \frac{f_{h,0,k}}{k_{90}\;sin^2\alpha + cos^2\alpha} \tag{3.5}$$

where

α = angle between the force and grain directions
$f_{h,0,k}$ = characteristic embedment strength parallel to fibre direction
k_{90} = correction factor for material type

In EC5 [14], the characteristic value of the yield moment for round steel bolts and dowels is determined using the relationship stated in 3.6:

$$M_{y,Rk} = 0.3\;f_u\;d^{2.6} \tag{3.6}$$

where

f_u is the tensile strength of the fastener

The withdrawal capacity, denoted as $f_{ax,k}$, of a screw relies on its threading. The determination of the withdrawal strength can be achieved through 3.7:

$$f_{ax,k} = 0.52\;d^{-0.5}\;l_{ef}^{-0.1}\;\rho_k^{0.8} \tag{3.7}$$

The characteristic withdrawal capacity in timber joints with threaded fasteners can be defined as in 3.8 [5]:

$$F_{\mathrm{ax},\alpha,Rk} = \frac{n^{0.9}\;f_{\mathrm{ax},k}\;d\;l_{\mathrm{ef}}\;k_d}{1.2\;\cos^2\alpha + \sin^2\alpha} \tag{3.8}$$

where

α is the angle between screw axis and grain direction ($\alpha \geq 30°$)
k_d is $\min(d/8; 1)$
n is the number of screws acting in the joint
d is the outer thread diameter.

The axial strength of a screw, represented as $F_{ax,Rk}$ in the Eurocode, should be the minimum of the characteristic withdrawal strength, $F_{ax,k}$ and the tensile strength F_{tens} of the fastener [5].

In EC5 [14] there is a formula that considers simultaneous shear and axial load for screws loaded perpendicular to the grain direction, known as the interaction formula labeled 3.9 [2].

$$\left(\frac{F_{ax,Ed}}{F_{ax,Rd}}\right)^2 + \left(\frac{F_{v,Ed}}{F_{v,Rd}}\right)^2 \leq 1 \tag{3.9}$$

where

$F_{ax,Ed}$ is the design axial stress
$F_{ax,Rd}$ is the design axial strength
$F_{v,Ed}$ is the design shear stress
$F_{v,Rd}$ is the design shear strength

3.3.2 Assessment of material properties

Given the diverse range of screws with varying steel properties, diameters, and threads, it is crucial to have screws assessed by a notified body. The results of this assessment are then declared by the manufacturer as characteristic values in a declaration of performance (DOP).
Alternatively, these values, essential for calculating the load bearing capacity of screwed joints, can be specified in a European Technical Assessment (ETA). Consequently, parameters crucial for joint design, including yield moment ($M_{y,k}$), withdrawal capacity ($f_{ax,k}$), and diameter (d) required for determining shear strength for modern screws, are stated in ETAs or declared by the manufacturer in DOPs.

Another notable aspect in ETAs is the consideration of torque moment. Screws often employ special drive systems, typically Torx, to achieve the required torque levels during insertion. However, it is crucial to ensure that these torque levels do not result in screw damage [2].

3.3.3 Stiffness

Comprehending joint behavior is essential for the design of timber framing. The slip modulus, represented as K_{ser} or $K_{SLS,v}$, is a parameter that reflects stiffness and can be derived from the load-displacement curves according to [22]. EC5 [14] offers an expression (3.10) for the slip modulus based on the numerical test results, applicable to bolted and dowelled joints under serviceability loads [2].

$$K_{ser} = \frac{d\,\rho_m^{1.5}}{23} \tag{3.10}$$

The value of the stiffness reported in 3.11 must be doubled for steel-to-timber joints. However, there are stiffness variations in different directions within a joint. Concerning self-tapping screws (STS), the current edition of EC5 [14] does not specify the method for calculating withdrawal stiffness. However, the subsequent draft of EC5 [23] incorporates the axial stiffness, $K_{SLS,ax}$, of STS in the serviceability limit state, where it is determined according to 3.11:

$$K_{SLS,ax} = 160\,\frac{\rho_m^{0.85}}{420}\,d^{0.9}\,l_w^{0.6} \tag{3.11}$$

In the case of joints featuring inclined STS, the upcoming revision of Eurocode 5 [23] defines K_{SLS} as the composite of $K_{SLS,v}$ and $K_{SLS,ax}$ as follows in 3.12

$$K_{SLS} = K_{SLS,v}\,sin\epsilon\,(sin\epsilon - \mu cos\epsilon) + \frac{1}{2}\,K_{SLS,ax}\,cos\epsilon\,(cos\epsilon + \mu sin\epsilon) \tag{3.12}$$

where

ϵ is the inclination of the fastener

μ is the coefficient of friction

Given that the load-displacement behavior of joints is nonlinear, stiffness diminishes as displacement increases. To accommodate this non-linearity in the ultimate limit state (ULS), the existing EC5 [14] specifies that the stiffness, K_u in ULS, can be considered as in 3.13:

$$K_u = \frac{2}{3}\,K_{SLS} \tag{3.13}$$

4

Previous investigations

Screws are particularly well-suited for handling significant withdrawal loads, making them the preferred choice for joints where fasteners are arranged in inclined or cross-wise configurations. In an inclined configuration, the screws endure biaxial stresses: along the screw axis (during withdrawal) and perpendicular to the screw axis (according to Johansen theory) [2]. This arrangement leverages the high load bearing capacity along the screw axis, enabling the creation of robust joints capable of bearing substantial loads. Typically, most of the load is carried longitudinally by the screws due to their greater stiffness compared to lateral loading scenarios. However, when screws are arranged at an angle, their lateral load bearing capacity is not considered. This is because the equations in EC5 [14] are applicable only to fasteners positioned perpendicular to the grain direction and therefore not suited for inclined screws.

The following chapter gives an overview of previous investigations within the research field of timber joints using inclined self-tapping screws.

4.1 Bejtka & Blass

The research conducted by Bejtka and Blass [24] is of significant importance in the field of inclined screws and timber. The authors carried out experiments using test specimens consisting of one central member and two side members, as depicted in Figure 4.1. These components were connected using one self-tapping screw for series 1 or four self-tapping screws for series 2, all featuring fully threaded screws. Furthermore, the screws had a diameter of 7.5mm and lengths of 130mm for series 1 and 180mm for series 2. The test specimens were constructed from glue-laminated timber with a moisture content set at 12%. Within each series, the specimens exhibited consistent density, averaging 400kg/m^3 for series 1 and 442kg/m^3 for series 2. In addition, each series was divided into sub-series. Series 1 comprised five sub-series, while series 2 comprised four sub-series, where parameters such as angle alpha ($0° - 50°$), timber thickness, and penetration depth varied.

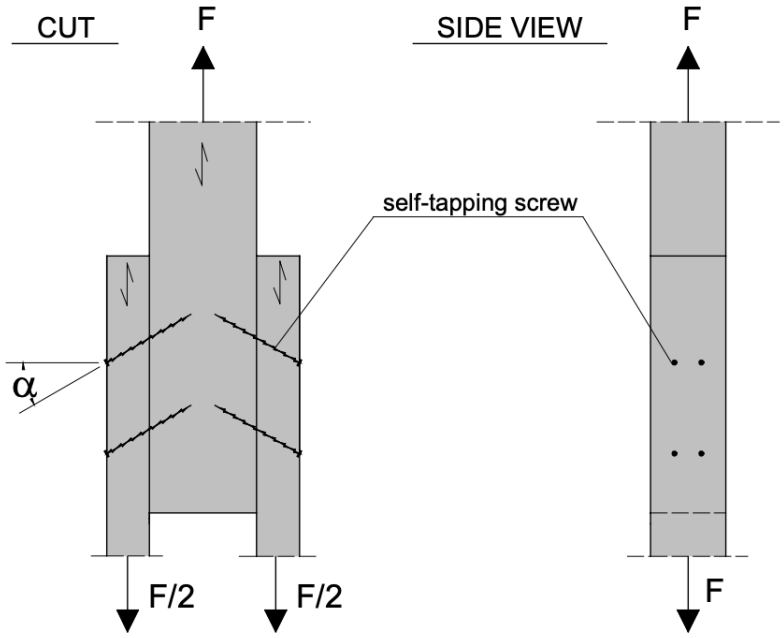

Figure 4.1: Bejtka & Blass testing configuration. [24]. Reprinted with permission.

Furthermore, Bejtka & Blass formulated a theoretical calculation model (4.1) for the load bearing capacity of connections based on the balance between the axial and lateral resistance, where ϵ is the load-to-screw axis angle and μ the coefficient of friction:

$$R = R_v\,(cos\epsilon - \mu\ sin\epsilon) + R_{ax}\,(sin\epsilon + \mu\ cos\epsilon) \tag{4.1}$$

4.2 Tomasi, Crosatti & Piazza

Further exploration into the research field of inclined screws was carried out by Tomasi et al. [25], aiming to validate calculation models specifically designed to describe the mechanical behavior of inclined screw joints, especially focusing on the load bearing capacity and stiffness of the joint. By incorporating the work of Bejtka and Blass [24] and the EC5 [14] quadratic interaction formula (3.9), a theoretical model for calculating the load bearing capacity was developed. The model is, according to the authors, suitable for inclined screws experiencing shear-tension stress, shear-compression stress, and a combination of both under an x-shaped position.

Tomasi conducted an experimental series on timber-to-timber connections, comprising 64 push-out tests, at the Department of Mechanical and Structural Engineering, University of Trento. The test specimens consisted of glue-laminated timber of the GL24h strength classification, with a moisture content of 12% and a specified wood density. The test configuration involved two lateral wood elements connected to a central member using self-tapping double-thread screws anchored at 0, 15, 30, and 45 degrees relative to the shear plane. Two different screw lengths were utilized, 190 and 220 mm. For connections at 0 and 15 degrees, 190mm screws were employed, whereas 220mm screws were used for those at 30 and 45 degrees. Throughout the tests, the specimens were subjected to compression stress, with displacements recorded via four linear variable differential transformers positioned in pairs on both sides of the samples along the shear plane, while load measurements were taken using load cells. A depiction of the test setup can be seen in Figure 4.2. .

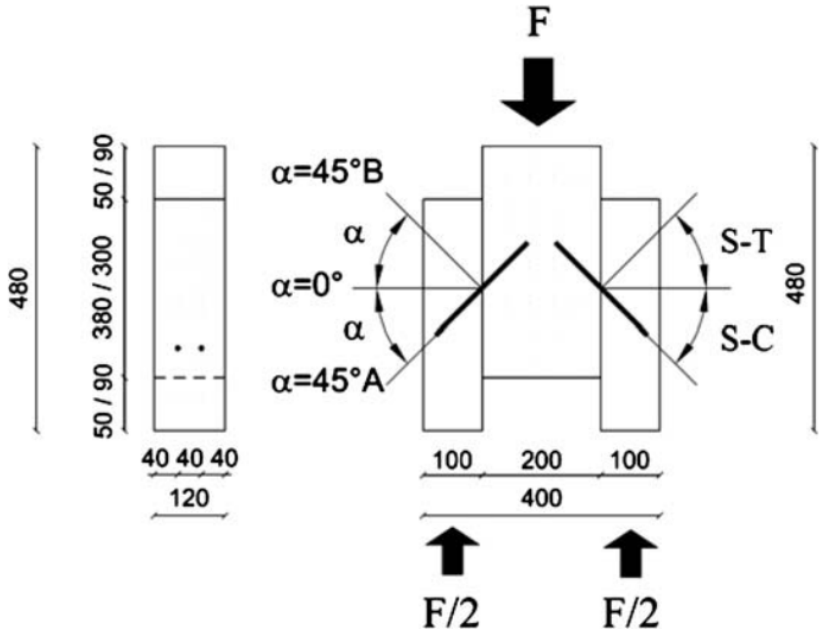

Figure 4.2: Experimental test set up. [25]. Reprinted with permission.

Through evaluation of the load-bearing capacity, Tomasi et al. [25] concluded that the EC5 [14] calculation method is generally unfavorable in terms of safety for screws subjected to shear compression loads. The equation (interaction formula) does not adequately predict the increase in load bearing capacity as the angle between the screw and the load increases. In contrast, it proves to be favorable in terms of safety when screws are subjected to shear-tension loads and placed in an X-shaped position. The authors also concluded that the calculation methods proposed in [25] ensure safety for all geometrical configurations tested.
In their assessment of joint stiffness, they found that the EC5 [14] calculation method offers an accurate estimation of the slip modulus when screws experience shear-compression loads perpendicular to the shear plane. However, when screws are arranged in a cross-shaped configuration, the formula underestimates the slip modulus and is therefore deemed entirely unsuitable. They formulated that the stiffness of the joints is the aggregate of both lateral and axial stiffness, as indicated in equation 4.2.

$$K_{\text{ser}} = K_{\perp}\ \cos\alpha\,(\cos\alpha - \mu\ \sin\alpha) + K_{\parallel}\ \sin\alpha\,(\sin\alpha + \mu\ \cos\alpha) \tag{4.2}$$

4.3 Jockwer, Steiger & Frangi

Jockwer, Steiger, and Frangi have also made contributions within the field of research, although slightly different from the test setup conducted in this thesis. In their paper [12], a design model was proposed to calculate the load bearing capacity and stiffness of inclined screws. Unlike Blass and Tomasi, Jockwer et al. conducted tests not only with forces parallel to the grain direction of the member ($\epsilon = 0°$) but also with a combination of parallel and perpendicular loads.

By incorporating the work of Bejtka and Blass, Jockwer et al. developed a calculation model that considers the effective embedment length of the screw, expressed as:

$$x_1 = \frac{f_h\ d_{ef}}{2\ tan\alpha\ f_{v,roll}} \tag{4.3}$$

Equation 4.3 implies that the complete embedment strength, f_h, is reached at a distance x_1 from the surface. Using this adjustment of the diminished embedment strength and employing Johansen's models, the lateral load bearing capacity of the screw, loaded perpendicular to the grain, is determined as follows:

$$R_{\perp} = -f_h\ x_1\ d_{ef} + \sqrt{(2\ M_y + f_h\ x_1^2\ d_{ef})\ f_h\ d_{ef}} \tag{4.4}$$

Concerning the stiffness of a joint, Jockwer et al. derived an equation for the lateral direction as:

$$K_{\perp} = \frac{3\ E_{steel}\ \pi\ d_{core}^4}{64\ x_1^3} \tag{4.5}$$

When loaded perpendicular to the grain, the stiffness of a joint acts in series, where K_{ser} equals the sum of the inverse values of the stiffness in the lateral and axial directions:

$$\frac{1}{K_{ser}} = \frac{1}{K_{\perp}} + \frac{1}{K_{\parallel}} \tag{4.6}$$

This differs from Tomasi's equation (4.2), which is derived for loads aligned parallel to the grain.

Regarding the test setup, two different configurations were employed, each with varying shank-to-grain angles, load-to-grain angles, and timber densities. In the setups, three test series were conducted with angles of $\alpha = 90$, 60, and 45 degrees, using both high and low timber densities.

The first test set-up, referred to as the "pulling test", involved applying a tension force perpendicular to the grain ($\epsilon = 90°$). The second setup, depicted in Figure 4.3, involved the application of a force parallel to the grain ($\epsilon = 0°$), similar to a block shear test. Throughout the tests, displacements were measured at a constant speed of load. The test specimens consisted of glue-laminated spruce timber with high and low densities, a known moisture content, and fully threaded self-tapping screws. In the shear test, 1.5mm thick Teflon foil was placed between the side and the central member to minimize frictional forces. However, in the pulling test, no Teflon foil was used.

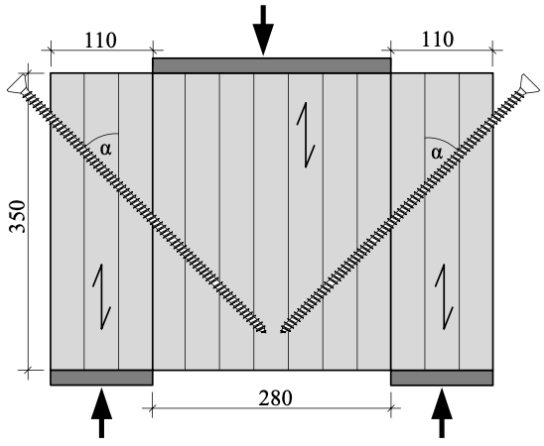

Figure 4.3: Jockwer, Steiger & Frangi test set-up illustration. [12]. Reprinted with permission.

Taking into account the results of the test series, the design methodologies evaluated in [12] yield lower load-bearing capacities for $\alpha = 90°$ degrees compared to the ultimate load achieved in the tests. According to the authors, the model that incorporates reduced embedment length is suitable when varying the angle alpha and provides a reliable estimate of the structural response of inclined screws loaded perpendicular to the grain direction. Consideration of the decreased embedment length allows for an accurate modeling of the significant decrease in stiffness. The authors also emphasize the importance of precise knowledge of the material properties used in the equation, rather than relying solely on the properties provided for dowel-type fasteners in EC5 [14].

4.4 Krenn & Schickhofer

Krenn & Schickhofer [11] performed and developed a test setup on inclined screws with steel plates as the outer member. Using glue-laminated timber and two different self-tapping screws, fully threaded and partially threaded, three series of tension tests were carried out. All tests were performed in the laboratory, using a displacement-controlled tension testing machine. In test series 1 and 2, the timber members were secured directly in the machine clamping device. However, for test series 3, a configuration involving steel tension rods and load-sharing plates was devised and tailored to fit the configuration of the testing machine. An illustration of the two test setups are provided in Figure 4.4.

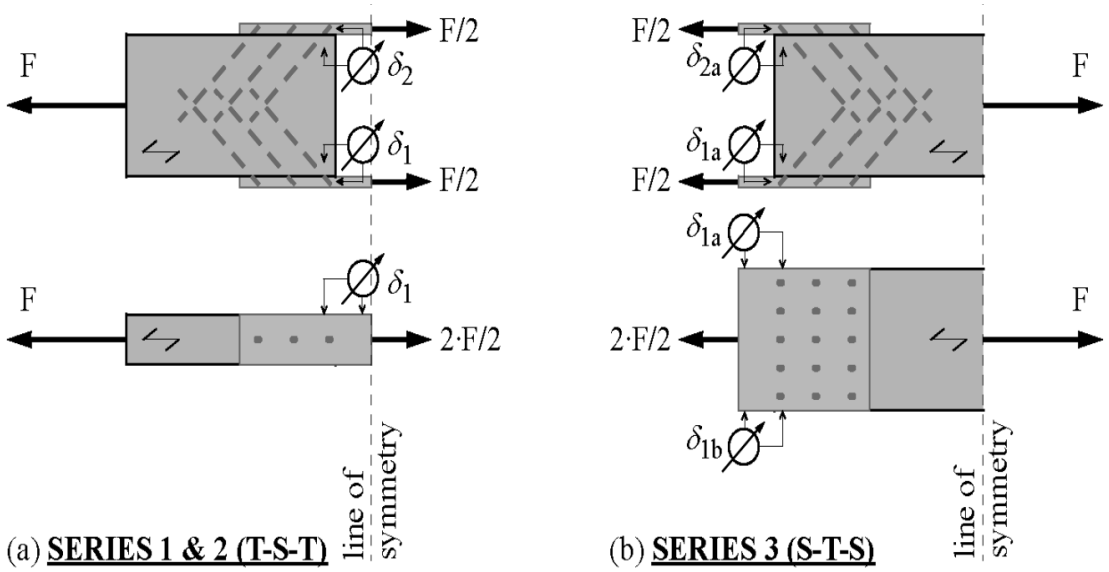

Figure 4.4: Krenn & Schickhofer testing configuration. [11]. Reprinted with permission.

The developed mechanical model, characterized as a truss model, demonstrated suitability to calculate the capacity of steel-to-timber joints and may be favored for its simplicity in design. This model integrates the axial load bearing capacity of the screw and the frictional forces at the interface between the timber member and the steel plate. The truss model is shown in Figure 4.5.

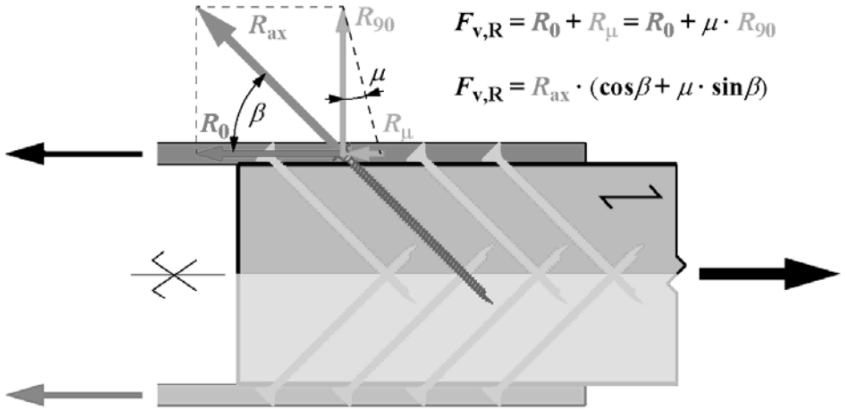

Figure 4.5: Krenn & Schickhofer Truss Model. [11]. Reprinted with permission.

4.5 De Santis et al.

De Santis et al. [26] conducted experimental investigations into steel-to-timber connections in seven different configurations, which involved varying shank-to-grain angles, interlayers, and specimen geometries. The tests consisted of standard push-out tests, in which the specimen consisted of a central timber member flanked by two outer steel members, as illustrated in Figure 4.5. The central timber member, constructed of GL24h spruce glue laminated timber, was tested to failure by a universal testing machine with a capacity of 100 kN. Relative displacement was measured using LVDT technology.

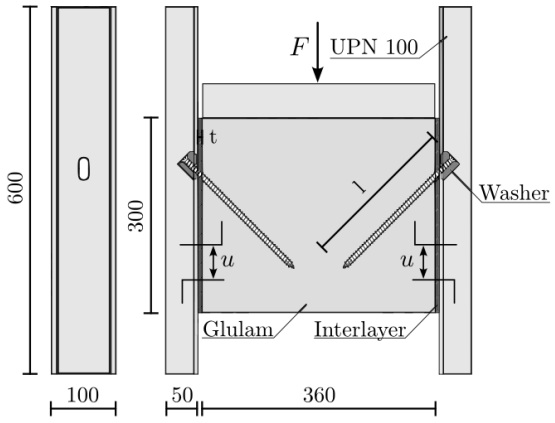

Figure 4.6: De Santis et al. experimental configuration. [26]. Reprinted with permission.

In their paper [26], De Santis et al. also compared hundreds of finite element analyses concerning predicted loads with analytical equations such as the quadratic formula mentioned in EC5 3.9, Blass and Bejtkas' quasi-additive formula 4.1, and a hybrid additive-quadratic interaction model [26].

The proposed finite element models are considered, according to the authors, valid representations for inclined screws and their behavior concerning failure modes and loads.

5
Experimental campaign

5.1 General description

Two testing configurations were used in the experimental campaign, one symmetric and one asymmetric. The parameters of influence investigated are screw axis angle, screw length, pre-tensioning force, and friction.

5.2 Test specimens

5.2.1 Timber

For the test series, a total of six spruce GLT GL30C grade beams were ordered with specifications according to the table 5.1. The weight of the beam was determined when the beams arrived at the Chalmers Structures Laboratory. Using a moisture meter, the moisture content was determined at 11.6%. For each cut of a test specimen, small samples were cut adjacently, which was later studied to determine both the mean density of the test specimen and the density of each individual lamella. The test sample was then stored in a climate controlled environment to ensure a specific moisture content of 12%.

Label	Section $[mm]$	Length $[m]$	Bulk Density $[kg/m^3]$
B_180	90x180	1.5	506
B1_255	90x225	3.2	492
B2_255	90x225	3.2	502
B3_255	90x225	3.2	485
B1_315	90x315	3	458
B2_315	90x315	3	474

Table 5.1: Specifications of timber beams for parametric testing series.

5.2.2 Self tapping screws

The self tapping screws (STS) selected for experimental testing, manufactured by WURTH with reference number WURTH SHR-SEKPF-FRT-VG-RW40-(A3K)-8X200/181 were ordered in lengths of 120, 200 and 400 mm.

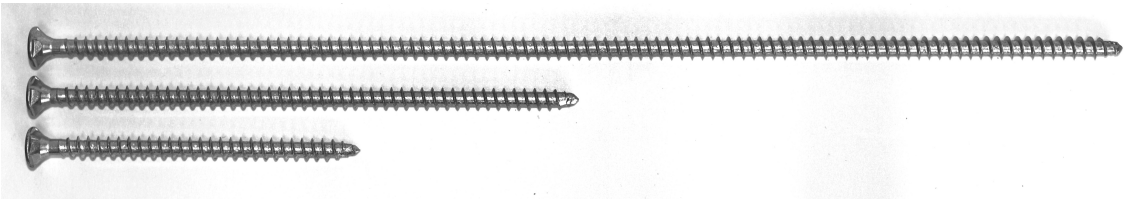

Figure 5.1: 120, 200, and 400 mm screws.

The specified geometrical and material characteristics of the screw according to ETA-11/0190 [27] are prescribed in Table 5.2. Joints within the WSH-subset (see Table 5.3) were to be assembled with a complementary angled washer intended for improved tensile force transfer, also provided by WURTH, reference number WNKLSHB-SE-45GRD-GUSS-A3K-85X4.

$d\ [mm]$	$f_{tens,k}\ [kN]$	$f_{tor,k}\ [Nm]$	$M_{y,k}\ [kNm]$
8	22	25	23

Table 5.2: Specifications of self tapping screws.

5.2.3 Steel plates

The steel plates for each test configuration were machined from 90x15mm S355 plate stock.

Figure 5.2: Steel plates machined for varying screw inclinations.

Initially, all plates were cut to the required length using a metal band saw. A 30 mm hole was drilled at the top of each plate to accommodate the load transfer pin that connects the specimen to the testing platform. For the 90-degree test configuration without the angled washer, an 8.5 mm hole was drilled and countersunk to allow the head of the self-tapping screw to seat correctly.

In the setup designed for the 45 degree screw angle tested with the aforementioned washer, a 10 mm slot was milled to properly seat the washer, see Figures 5.3 and 5.4. For tests involving 45- and 60-degree angles without the angled washer, additional machining was required to accommodate the drilling and countersinking processes. A relief cut was made using an end mill to create a flat cutting surface for a spiral and countersink drill bit (Figure 5.2).

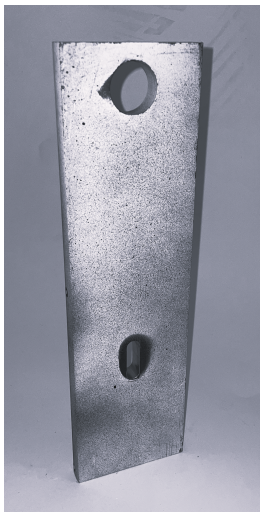

Figure 5.3: Steel plate with machined slot to seat angled washer.

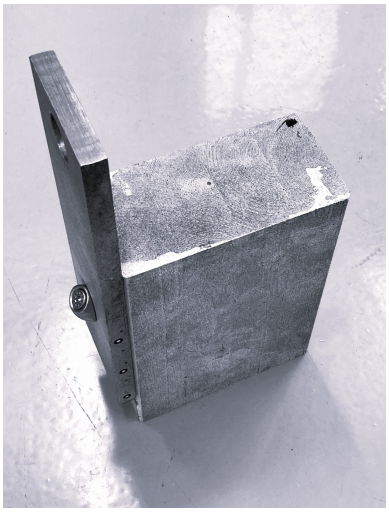

Figure 5.4: Specimen from set ASY_WSH_L200_A45_PF0_F0 assembled with
angled washer and STS.

5.2.4 Assembly and preparation

For the assembly process, a 3 mm spiral drill was used for pre-drilling the timber member. This step was performed before attaching the STS screw to ensure that no splitting occurred in the timber and to facilitate the correct angle and placement. Templates were created for 45, 60, and 90 degrees of shank-to-grain angle, shown in Figures 5.5 and 5.6. These templates were designed in AutoCad Inventor and then manufactured using a 3D printer at Chalmers University. The screws were then driven using a simple screw guide (Figure 5.7), at the correct angles into the timber using a battery-powered drill. Just before the screw head reached the steel plate, the drill was stopped and a torque wrench was used to ensure the appropriate pre-tensioning moment, M_{tors}, of either 0, 5, 15 or 22 Nm. To evaluate the friction parameter, a 1.5mm Teflon foil was inserted between the timber and steel plate before the members were screwed together. Finally, to prepare for Digital Image Correlation, the surfaces of the timber and steel members were coated with a stochastic speckled pattern. This involved first applying a solid white base layer using spray paint, followed by a light misting of black paint to create the pattern shown in Figure 5.9.

Figure 5.5: Guide for proper placement and inclination of pre-drilling.

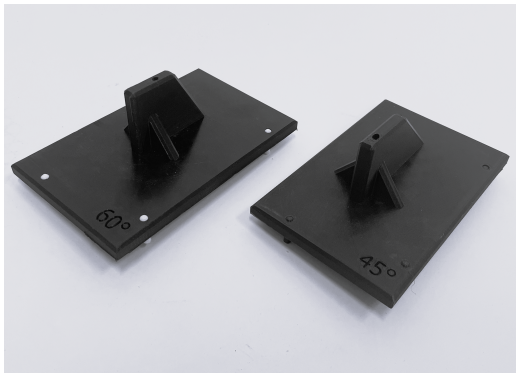

Figure 5.6: Guides for 60- and 45 degree pre-drilling.

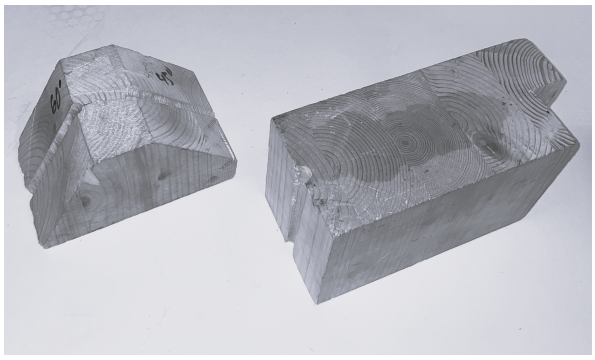

Figure 5.7: Guides for mounting screws at 45-, 60- and 90- degree angles.

Figure 5.8: Specimen with mounted steel plate with 90° screw angle.

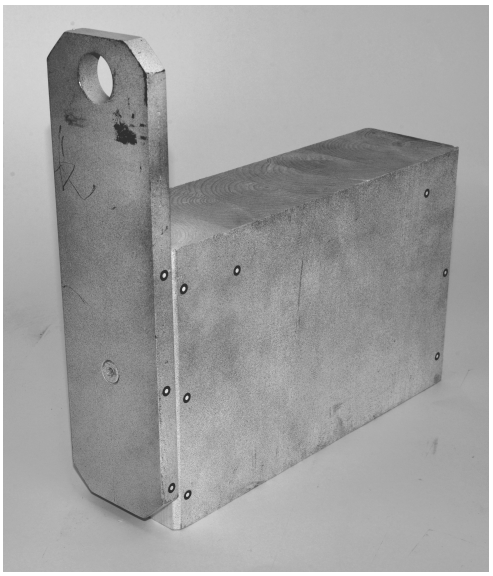

Figure 5.9: Specimen with applied surface pattern and markers.

5.3 Test set-up

The test setup for the parametric series, which involved asymmetric (Figure 5.11) and symmetric configurations (Figure 5.12), was designed to exert tension on the steel plate attached to one side of the timber specimen (asymmetric) or both (symmetric). Fixing the specimen to the machine work table involved clamping it down with a steel plate fastened by four 16mm threaded rods to a mounting plate secured to the T-slots of the test machine work table. The load application was carried out using a servohydraulic test machine, conducting the tests with displacement control at a speed of 1 mm/min until failure was reached. The load in the joints was first applied up to 40% of the estimated maximum load, then decreased to 10% of the predicted maximum load. This level was kept for some seconds and then loaded up to failure as depicted in figure 5.10. This was done to ensure full contact between the joint and the timber specimen and according to the standards EN 12512 [22] and EN 26891 [28]. Joint failure was defined as screw tensile failure (screw head tear-off), load dropping to 50 % of F_{ult}, alternatively reaching a maximum displacement of 15 mm (withdrawal).

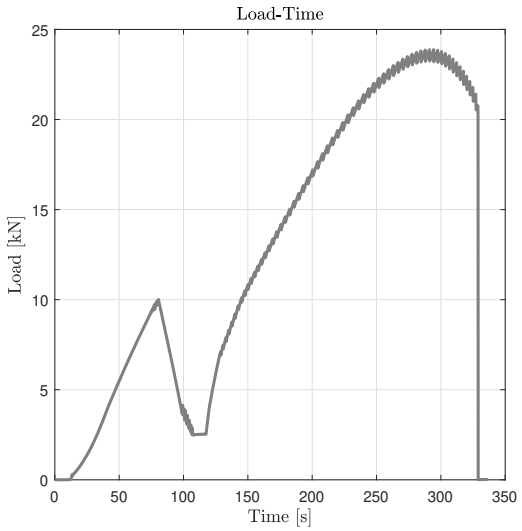

Figure 5.10: Load/Time relationship.

In the asymmetric testing configuration, load measurements were captured by a 220 kN load cell connected to the control system of the testing machine. DIC images were synchronized with load values obtained from the load cell and testing apparatus to generate the load-displacement relationship during the duration of the test sequence.

In the symmetric test setup, two 50 kN capacity load cells were used to measure loads on each steel plate positioned on either side of the timber specimen. The primary 220 kN load cell remained attached to the machine, connected to the two smaller cells through a rig manufactured from water jet cut S355 steel profiles with machined attachment points. These smaller cells, attached to the steel profile, were hinged for flexibility and load distribution with similar load distribution pins as in the asymmetric configuration. The experiment ended when one of the two joints failed and the opposite side of the specimen would be subsequently tested until failure. The overview of the tested specimens is given in Table 5.3.

Label	Section [mm]	Height [mm]	α [°]	l [mm]	M_{tors}	Friction type	Repetitions
ASY_WSH_L200_A45_PF0_F0	90X225	320	45	200	15	S-T	3
ASY_WSH_L120_A45_PF0_F0	90X180	250	45	120	5	S-T	3
ASY_WSH_L400_A45_PF0_F0	90X225	450	45	400	15	S-T	3
ASY_L200_A45_PF0_F1	90X225	320	45	200	15	T	3
ASY_L200_A90_PF0_F0	90X315	200	90	200	15	S-T	3
ASY_L200_A90_PF1_F0	90X315	200	90	200	22	S-T	3
ASY_L200_A90_PF2_F0	90X315	200	90	200	0	S-T	3
ASY_L200_A60_PF0_F0	90X225	200	60	200	15	S-T	3
SYM_L200_A90_PF0_F0	90X315	200	90	200	15	S-T	3
SYM_L200_A45_PF0_F0	90X225	200	45	200	15	S-T	3

Table 5.3: Test specimen specifications for the parametric test series
S-T for Steel-to-Timber interaction and T for steel-Teflon-timber interaction.

where label entries entail

ASY	Asymmetric Configuration
SYM	Symmetric Configuration
WSH	45° degree washer
L	Screw length
A	Screw angle
PF	Pre-tensioning type
F	Friction type

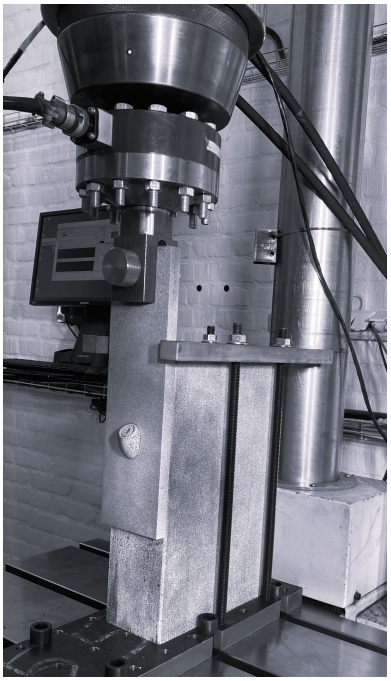

Figure 5.11: Asymmetric test setup.

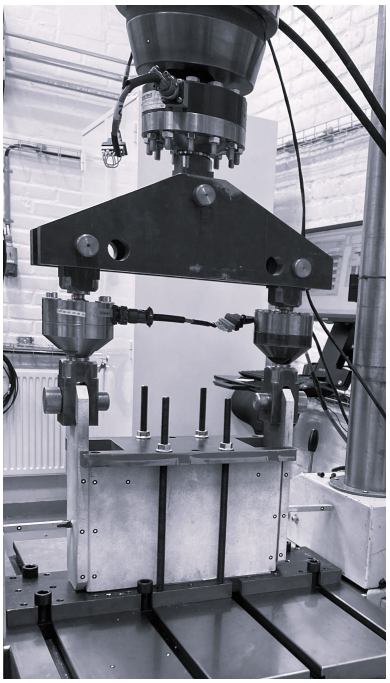

Figure 5.12: Symmetric test setup.

5.4 Measurements/Data collection

The data collection method chosen for the experimental investigation was Digital Image Correlation (DIC). DIC is an optical technique that measures displacement and strain on the surfaces of objects subjected to mechanical loading. This section provides a brief description of the technology, its principles, and its adaptation for this study.

5.4.1 Digital Image Correlation (DIC)

During most of the experimental campaign, DIC technology was used to capture various displacements of the specimens (Figure 5.13). DIC, which is an optical and non-contact method, facilitates the registration of changes in 2D and 3D digital image sequences by tracking the movement of the pixels [29]. This method requires either a stochastic, speckled pattern or markers on the surface of interest to depict discrete image areas. By comparing the positions of these markers in images acquired before and during deformation, the software can determine displacements at various locations on the object, typically represented as a vector quantity indicating both the magnitude and the direction of movement. In the context of this experimental campaign, the DIC process consisted of several stages: pattern application, reference image acquisition, pattern and marker recognition, image capture, and data extraction.

To evaluate alterations in shape and motion, a set of cameras was calibrated to capture high-resolution images before, during, and after the test. These images undergo various processing methods to enhance their quality and minimize any adverse effects that could disrupt tracking.

Using GOM Correlate 2018 digital image correlation software, the relevant data was extracted and presented visually using MATLAB-generated plotted graphs.

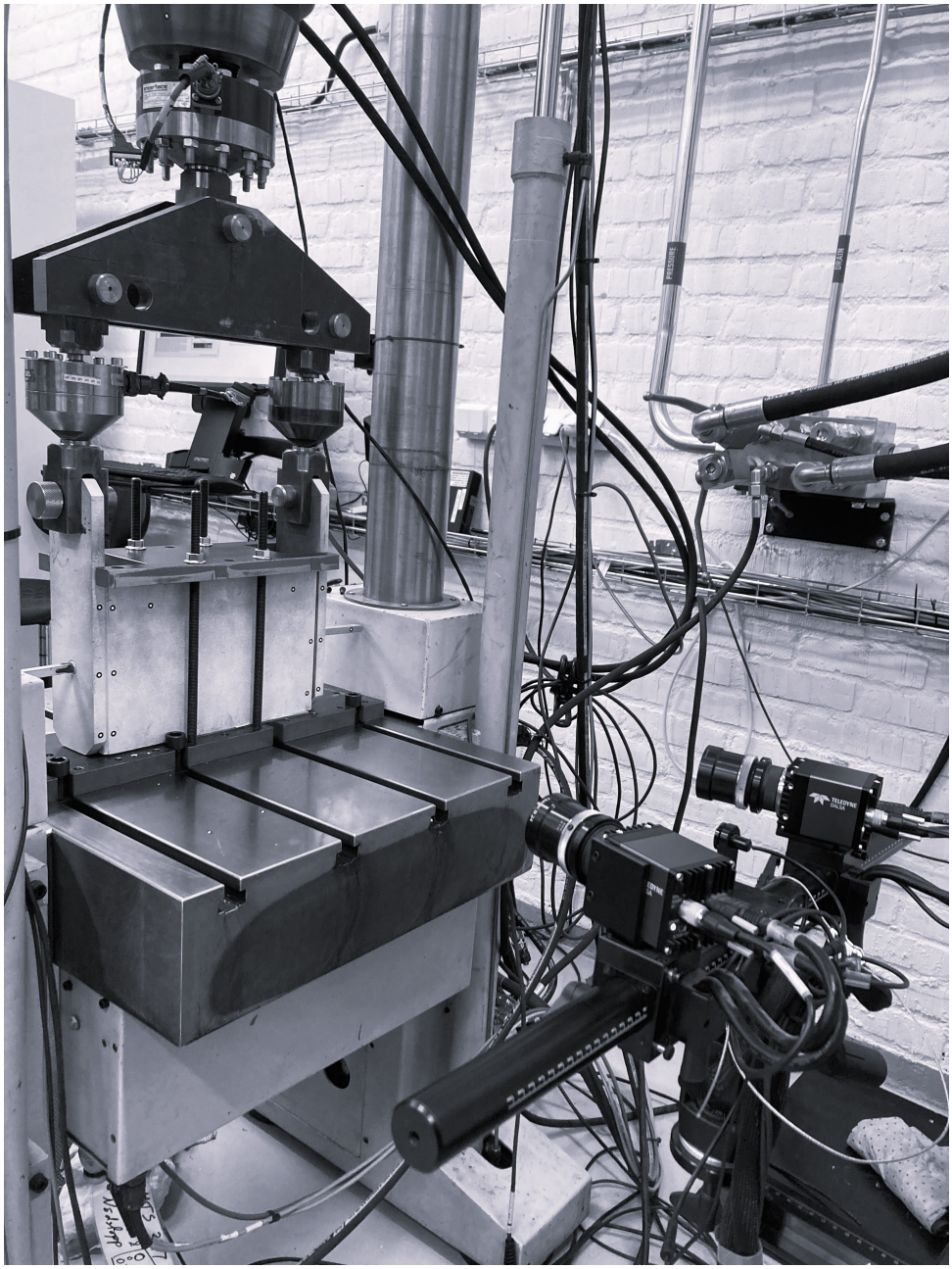

Figure 5.13: DIC camera setup for symmetric test configuration.

6
Results and discussion

The following chapter presents the findings of the experimental campaign. The results selected from the experimental campaign are illustrated in representative graphs plotted in MATLAB. The displacement of the joints, sometimes referred to as slip, is defined as the displacement of the steel plate subtracted with the displacement of the timber member, resulting in the relative displacement of the steel member. The graphs depict the various parameters examined, including screw inclination, screw length, pretensioning moment, and friction type.

The subsequent discussion provides a description of the load-displacement curves, along with a discussion of the experimental campaign procedure.

6.1 Results

The representative load-displacement curves for the experimental campaign are presented in Figures 6.1 - 6.4. Throughout the experimental campaign, different parameters were examined, resulting in variation of failure modes and failure loads illustrated in Table 6.1. Initially, some of the joints tested exhibited initial slip. Possible explanations for this characteristic are inadequate contact between the timber member and the steel plate, material imperfections, and assembly processes that could affect load transmission.

During the phase immediately following the initial slip, known as the first loading phase, the joint demonstrated its highest stiffness. This phase often displays linear behavior. Before reaching maximum load, the curve exhibits discontinuities. These unloading and reloading cycles almost demonstrates linear elastic behaviour, with a stiffness in these regions that is larger than the maximum stiffness of the first loading phase.

As the load reaches a plateau, the stiffness of the joints decreases. Failure modes in this region typically involve withdrawal failure and high ductility. The decrease in stiffness correlates with the compression strength of the timber for a 45-degree screw inclination; however, for an inclination of 90 degrees, we can see that the curves exhibit a hardening effect because of the formation of a plastic hinge. The failure modes in our experimental campaign involved screw head tear-off for 90- and 60-degree inclinations, and for a inclination of 45 degrees, both screw head tear-off (HTO) and withdrawal failure (WITH) occurred. Examples of these types of failure are depicted in Figure 6.1 where HTO failure is characterized by a sudden decrease

in load with little to no further displacement, indicating a less ductile failure of the screw has occurred. A Withdrawal failure is identified by its larger deformation and gradual decrease in load, signifying that the fastener is being withdrawn from the specimen.

Label	$\mathbf{F}_{ult}$ [kN]	Failure
ASY_WSH_L120_A45_PF0_F0_R1	9.5	WITH
ASY_WSH_L120_A45_PF0_F0_R2	11.3	WITH
ASY_WSH_L120_A45_PF0_F0_R3	13.0	WITH
ASY_WSH_L200_A45_PF0_F0_R1	21.7	WITH
ASY_WSH_L200_A45_PF0_F0_R2	20.0	HTO
ASY_WSH_L200_A45_PF0_F0_R3	22.5	HTO
ASY_WSH_L400_A45_PF0_F0_R1	20	HTO
ASY_WSH_L400_A45_PF0_F0_R2	22.5	HTO
ASY_WSH_L400_A45_PF0_F0_R3	21	HTO
ASY_L200_A45_PF0_F0_R1	⋆	⋆
ASY_L200_A45_PF0_F0_R2	⋆	⋆
ASY_L200_A45_PF0_F0_R3	24.8	HTO
ASY_L200_A45_PF0_F1_R1	20.4	HTO
ASY_L200_A45_PF0_F1_R2	20.3	HTO
ASY_L200_A45_PF0_F1_R3	22.5	HTO
ASY_L200_A90_PF0_F0_R1	12.5	HTO
ASY_L200_A90_PF0_F0_R2	11.8	HTO
ASY_L200_A90_PF0_F0_R3	10.7	HTO
ASY_L200_A90_PF1_F0_R1	15.3	HTO
ASY_L200_A90_PF1_F0_R2	14.6	HTO
ASY_L200_A90_PF1_F0_R3	13.8	HTO
ASY_L200_A90_PF2_F0_R1	13.8	HTO
ASY_L200_A90_PF2_F0_R2	14.0	HTO
ASY_L200_A90_PF2_F0_R3	⋆	HTO
ASY_L200_A60_PF0_F2_R1	⋆	HTO
ASY_L200_A60_PF0_F2_R2	20.5	HTO
ASY_L200_A60_PF0_F2_R3	⋆	HTO
SYM_L200_A90_PF0_F0_R1	13.5	HTO
SYM_L200_A90_PF0_F0_R2	⋆	HTO
SYM_L200_A90_PF0_F0_R3	⋆	HTO
SYM_L200_A45_PF0_F0_R1	⋆	⋆
SYM_L200_A45_PF0_F0_R2	23.6	WITH
SYM_L200_A45_PF0_F0_R3	⋆	⋆

Table 6.1: Representation of ultimate load value and failure mode of experimental campaign.

where

WITH	Withdrawal failure
HTO	Head tear-off failure
$\mathbf{F}_{ult}$	Maximum load value extracted from the load cell data.
⋆	Results omitted due to time limitations and/or testing failure.

6.2 Discussion

6.2.1 Load displacement behavior

Variation in screw length

Figure 6.1 depicts various lengths of screws: 120 mm, 200 mm, and 400 mm, all at a fixed angle of 45 degrees. As shown in the figure, the load bearing capacity is practically the same for 200- and 400-mm screws in this set-up, the failure modes are both head tear off and the joint capacity is connected to the tensile capacity of the screw. However, for the 120mm length, a more ductile behavior due to the withdrawal failure mode can be observed.

Considering stiffness, denoted as K_{ser}, which is calculated as the slope within the range of $0.1F_{ult}$ and $0.4F_{ult}$ according to EN 12512 [22], the screw length parameter does not appear to have a significant influence on stiffness. This is also confirmed with equation 3.10 for the stiffness in serviceability limit state in EC5 [14], which only includes the diameter of the fastener and the mean density of the timber.

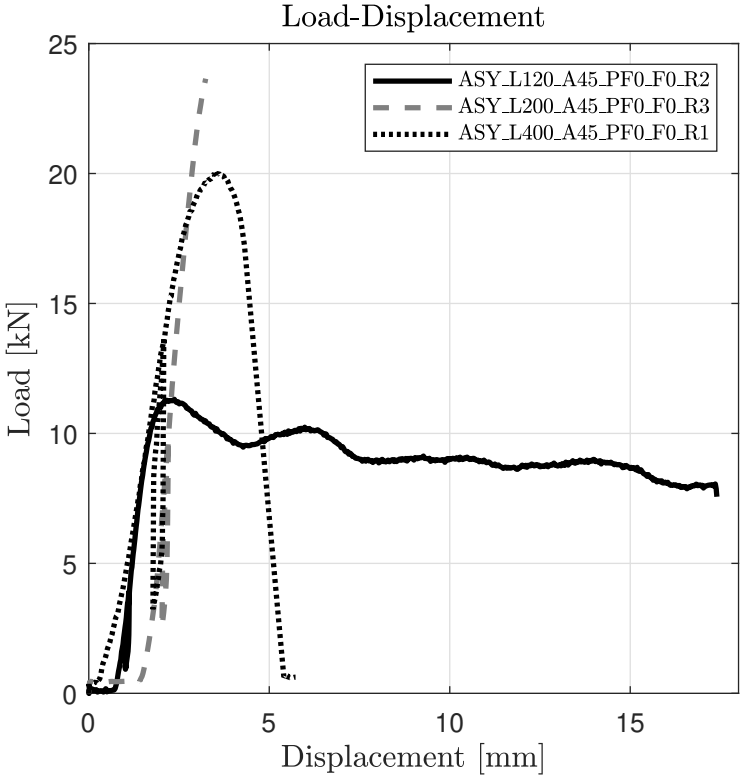

Figure 6.1: Comparative plot with representative tests with varying screw length.

The screw length parameter appears to have an influence on the load-carrying capacity for screws arranged at a 45-degree inclination. This is because the withdrawal strength is greater than the tensile strength for longer screws and the tensile strength is higher than the withdrawal strength for shorter screws. Consequently, the failure mode corresponds to head tear-off, and a brittle failure is expected for longer screws.

Variation in pre-tensioning moment

In Figure 6.2, the load-displacement curve of the pretensioning moment parameter is illustrated, displaying varying moments of 0, 15, and 22 Nm. As depicted in the figure, 22 Nm in pretensioning has the highest load-carrying capacity.

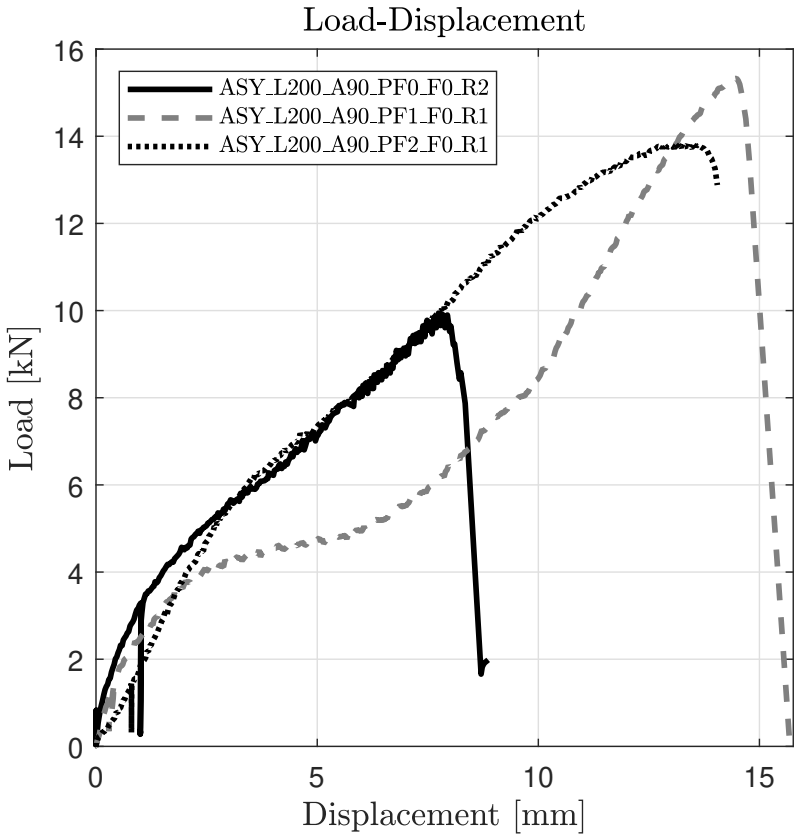

Figure 6.2: Comparative plot with representative tests with varying pre-tensioning moment.

Varying screw-to-grain angle

Figure 6.3 illustrates the impact of screw angle on the load-displacement curve. The highest load-bearing capacity is observed to be achieved at a 45-degree angle. This outcome is anticipated because as the screw experiences greater axial loading, its stiffness and capacity increase, benefiting from the screw's high withdrawal capacity. The outcome also corresponds well to 4.1 which states that the resistance of a connection is based on the balance of axial and lateral resistance. In terms of stiffness within this configuration, the screw positioned at 45 degrees exhibits the highest stiffness. Regarding ductility, it is lower for an inclination of 45 degrees compared to a 90 degree inclination. This is because for 90 degrees the ductility from the plastic hinge development can be taken into account before reaching the brittle failure of the screw head, this is special for steel-to-timber joints when the screw head is fixed within the steel plate.

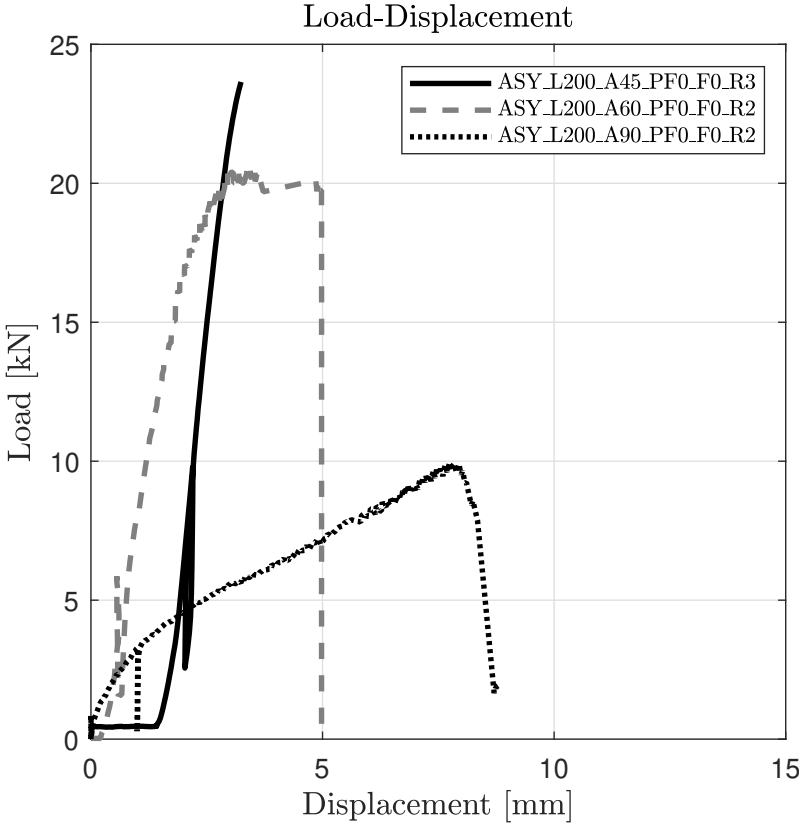

Figure 6.3: Comparative plot with representative tests with varying screw-to-grain angle.

Test configuration comparison

Figure 6.4 represents a comparison between the asymmetric and symmetric test setup, with the same angle, screw length, and pretensioning moment. The two load-displacement curves are similar and therefore comparable.

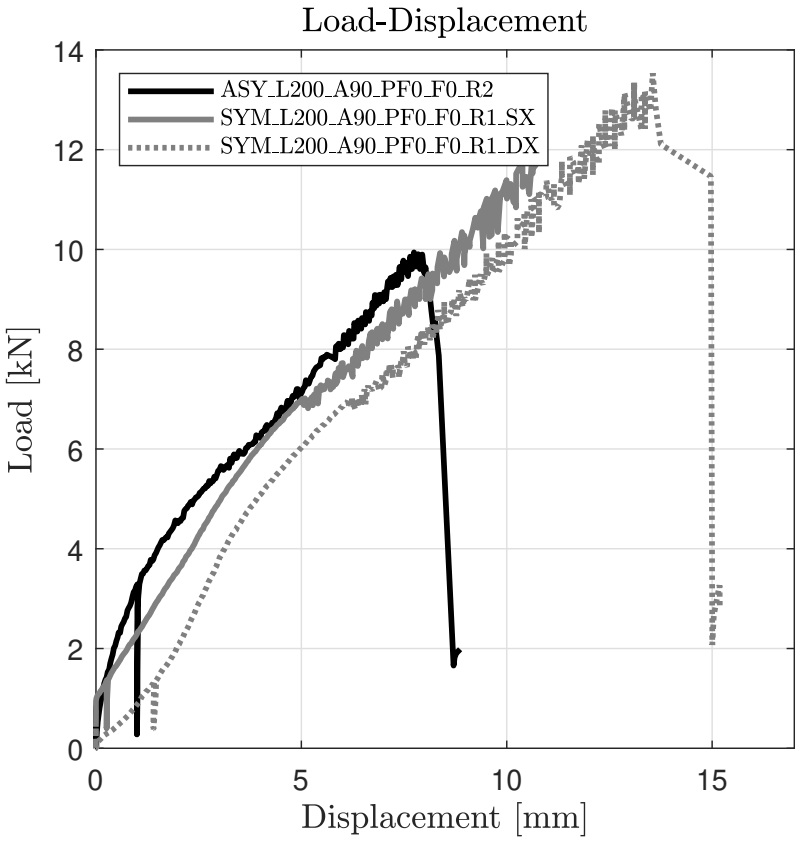

Figure 6.4: Comparative plot of representative results with varying test configuration at 90 degrees screw/grain angle.

6.2.2 Material and methods

Digital Image Correlation (DIC) was generally effective in collecting data on load-displacement behavior. However, there were issues with effectively detecting the surface pattern and markers on the specimen, most likely due to calibration issues, resulting in challenges associated with acquiring the correct depth of focus when measuring in two angled planes.

For the preparation of the timber samples, 50mm pieces were cut at one end of the each timber specimen. This was done to track the density profile and to decide on the most appropriate screw mounting side. The density was calculated using the classical relationship between the mass and volume. However, the definite screw mounting side was also governed by anomalies such as knots and finger joints. In general, considering the anisotropy of the timber, the most appropriate side to mount the screw on the timber is an uncertain variable that could have an effect on the behavior of the tested joints.

The servo-hydraulic load frame used in the tests is deemed suitable for joint testing. The machine was easy to use and the testing methodology aligned well with the procedures used by other researchers. However, different configurations could be explored in the future to further investigate joint behavior. Alternative methods to evaluate joints could include Finite Element Analysis (FEA) which may provide insights into stress distribution and failure mechanisms of joints.

7
Conclusion and future work

7.1 Conclusion

In this paper, an experimental investigation is conducted on timber-to-steel joints, using steel plates and STS screws, aiming to deepen the understanding of these joints in terms of behavior, load-carrying capacity, and stiffness. The paper also includes a review of relevant literature to deepen the understanding of timber and steel as materials. Subsequently, the focus shifted towards addressing timber joints, their behavior, and design in accordance with the current design code. Furthermore, the review examined previous research on inclined self-tapping screws, with a particular emphasis on the test setup and various analytical models.

During the experimental campaign, various parameters that could affect the load-displacement curve of steel-to-timber joints were tested. These parameters included screw inclination, fastener length, pretensioning moment, and friction type. The tests provided insights into the effects of these parameters on the load-displacement relationship. The main conclusion that can be drawn from the thesis and its experimental campaign is that these parameters have a distinct effect on the load-displacement curves. The highlighted parameters are important to take into account when designing steel-to-timber joints with self-tapping screws.

Taking into account the influence of the angle, the more the screw is loaded in the axial direction, the higher the load carrying capacity and stiffness. This emphasizes that the angular distribution is important for the optimization of joints. The screw length seems also to affect the load-displacement curve with different load-carrying capacities for different lengths. but also different failure modes.

When it comes to the pretensioning moment, this parameter do also effect the load-displacement behaviour in the configuration involved in the thesis. However, high torque levels should be used conservatively to avoid damaging the screw.

One of the main research questions in this thesis was to see whether an asymmetric test setup is feasible in joint testing. Conclusions could be drawn that the load-displacement curves do look similar in comparison with the symmetric setup, although this asymmetric configuration should be further evaluated in future research.

During the experimental testing, it was observed that measurement techniques such as Digital Image Correlation (DIC) and LVDT are convenient tools for evaluating joint behavior. The test apparatus performed well and corresponds to previous test procedures within steel-to-timber joints.

The use of timber in construction is widely recognized for its environmental benefits, compared to traditional materials like concrete and steel. Incorporating innovative joint techniques, such as inclined self-tapping screws, can enhance the sustainability of timber structures by reducing the need for metal connectors and adhesives, which often have big environmental footprints. Timber, being a renewable resource, reduces environmental impact when sourced from sustainably managed forests. The screws used in this study are efficient and durable, promoting the longevity and integrity of timber structures.

7.2 Future work

The experimental campaign only explored a limited selection of configurations and connection parameters. Future endeavors could focus on expanding the scope to encompass a broader range of configurations and parameters, such as material properties, environmental factors, and different joint geometries.

Experimental testing of the variability of the load-displacement behavior could also be conducted in future investigations. Such endeavors would contribute to a more comprehensive understanding of timber-to-steel joints and enhance the applicability of the findings in practical engineering applications.

Future studies could also incorporate a combination of experimental testing, FEA, and analytical modeling to provide a holistic understanding of joint behavior and improve the reliability of design recommendations. Additionally, regarding sustainability, a life-cycle assessment (LCA) of timber joints with inclined self-tapping screws could provide a more comprehensive understanding of potential environmental benefits. Quantifying the reductions in embodied carbon and other environmental impacts associated with these joints.

7.3 Credits

It is important to highlight that the experimental campaign described in this thesis is part of an ongoing research project led by Ph.D. student Dorotea Caprio and A/Prof Robert Jockwer at Chalmers University of Technology. The authors of this thesis were participants in their research, that is, they did not participate in data analysis, calculations to predict failure modes, or assessments of predicted load carrying capacity. In addition, the authors were not part of the preparation for the experimental campaign, which means that they did not decide which parameters to evaluate, no orders or evaluations of the material used, and in general no participation in the decision-making processes. Furthermore, the authors participated in some experiments among many that were conducted. To further elaborate this, Caprio was responsible for most of the project, which means calculation of predicted failure loads and modes, evaluation, and quality assurance of the testing procedure and data acquisition. The load-displacement data was retrieved by Caprio. The students in this thesis participated in the specimen assembly process and were observant during the experimental campaign.

Bibliography

Book sources

[1] K. Zwerger, *Wood and Wood Joints: Building Traditions of Europe, Japan and China*. Berlin, Boston: Birkhäuser, 2023. DOI: doi:10.1515/9783035624847. (visited on 04/22/2024).

[2] H. J. Blaß and C. Sandhaas, *Timber Engineering - Principles for Design*. Karlsruhe: KIT Scientific Publishing, Sep. 2017, 658 pp. DOI: 10.5445/KSP/1000069616.

[3] M. Johansson, "Structural properties of sawn timber and engineered wood products," in *Design of timber structures - Structural aspects of timber construction*, E. Borgström, Ed., 2:2016., pp.26-68, vol. 1, 3 vols., Stockholm: Swedish Forest Industries Federation Swedish Wood, Oct. 2016, ISBN: 978-91-980304-8-8. [Online]. Available: https://www.svenskttra.se/siteassets/5-publikationer/pdfer/design-of-timber-structures-1-2016.pdf.

[4] M. Al-Emrani, M. Johansson, P. Johansson, and B. Engström, *Bärande konstruktioner Del 2*, Omarb. uppl. Göteborg: Institutionen för Bygg- och miljöteknik, Avdelningen för konstruktionsteknik, Chalmers tekniska högskola, 2011.

[5] H. Lindelöw, "Design of timber joints," in *Design of timber structures - Structural aspects of timber construction*, E. Borgström, Ed., 2:2016., pp.112-147, vol. 1, 3 vols., Stockholm: Swedish Forest Industries Federation Swedish Wood, Oct. 2016, ISBN: 978-91-980304-8-8. [Online]. Available: https://www.svenskttra.se/siteassets/5-publikationer/pdfer/design-of-timber-structures-1-2016.pdf.

Other sources

[6] I. F. C. Smith and M. Snow, "Timber: An ancient construction material with a bright future," *Forestry Chronicle*, vol. 84, pp. 504–510, 2008. [Online]. Available: https://api.semanticscholar.org/CorpusID:83623559.

[7] A. Teischinger, "Teischinger, a. (2016): Opportunities and limits of timber in construction. wood design focus, 26(4), 23-26; ISSN 1066-5757," *Wood Material Science and Engineering*, vol. 26, pp. 23–26, Jan. 2016.

[8] M. Schweigler, T. K. Bader, G. Hochreiner, and R. Lemaître, "Parameterization equations for the nonlinear connection slip applied to the anisotropic embedment behavior of wood," *Composites Part B: Engineering*, vol. 142,

pp. 142–158, 2018. DOI: https://doi.org/10.1016/j.compositesb.2018.01.003.

[9] Adolf Würth GmbH. "Timber construction using baubuche." (), [Online]. Available: https://media.wuerth.com/stmedia/wuerth/documents/documents/LANG_en/32412020.pdf.

[10] L.-M. Ottenhaus, R. Jockwer, D. v. Drimmelen, and K. Crews, "Designing timber connections for ductility – a review and discussion," *Construction and Building Materials*, vol. 304, p. 124 621, 2021. DOI: https://doi.org/10.1016/j.conbuildmat.2021.124621.

[11] H. Krenn and G. Schickhofer, "Joints with inclined screws and steel plates as outer members," in *International Council for Research and Innovation in Building and Construction, Working Commission W18 - Timber Structures, Meeting*, ., 2009, pp. 42–7–2, 1–42–7–2, 12.

[12] R. Jockwer, R. Steiger, and A. Frangi, "Fully threaded self-tapping screws subjected to combined axial and lateral loading with different load to grain angles," in *RILEM Bookseries*, vol. 9, Oct. 2013, pp. 265–272. DOI: 10.1007/978-94-007-7811-5_25.

[13] J. Köhler, "Reliability of timber structures," 2007. [Online]. Available: https://api.semanticscholar.org/CorpusID:114223044.

[14] European Committee for Standardization, *EN 1995-1-1: Eurocode 5: Design of timber structures - part 1-1: General - common rules and rules for buildings*, Brussels, Belgium, 2004.

[15] K. W. Johansen, "Theory of timber connections," 1949. [Online]. Available: https://api.semanticscholar.org/CorpusID:222413671.

[16] H. Krawinkler, "Loading histories for cyclic tests in support of performance assessment of structural components," 2009. [Online]. Available: https://api.semanticscholar.org/CorpusID:6444560.

[17] European Committee for Standardization, *EN 384:2016, structural timber - determination of characteristic values of mechanical properties and density*, Brussels, Belgium, 2016.

[18] European Committee for Standardization, *EN 408:2010, timber structures - structural timber and glued laminated timber - determination of some physical and mechanical properties*, Brussels, Belgium, 2010.

[19] D. Caprio, "Consideration of the non-linear behaviour of joints for efficient design of complex timber structures," Ph.D. dissertation, Chalmers University of Technology, Department of Architecture and Civil Engineering, 2023. [Online]. Available: https://books.google.se/books?id=1GTgzwEACAAJ.

[20] Rothoblaas. "Smartbook timber screws." (May 2, 2023), [Online]. Available: https://issuu.com/rothoblaas/docs/smartbook-timber-screws-en.

[21] M. Dorn, K. d. Borst, and J. Eberhardsteiner, "Experiments on dowel-type timber connections," *Engineering Structures*, vol. 47, pp. 67–80, 2013. DOI: https://doi.org/10.1016/j.engstruct.2012.09.010.

[22] European Committee for Standardization, *EN 12512:2001: Timber structures - test methods - cyclic testing of joints made with mechanical fasteners + a1 (2005)*, Brussels, Belgium, 2001.

[23] European Committee for Standardization, *prEN 1995-1-1: Eurocode 5 design of timber structures — part 1-1: General rules and rules for buildings. CEN/TC 250/SC 5 n 1650.* Brussels, Belgium, 2004.

[24] I. Bejtka and H. J. Blass, "Joints with inclined screws," 2002. [Online]. Available: https://api.semanticscholar.org/CorpusID:136119828.

[25] R. Tomasi, A. Crosatti, and M. Piazza, "Theoretical and experimental analysis of timber-to-timber joints connected with inclined screws," *Construction and Building Materials*, vol. 24, no. 9, pp. 1560–1571, 2010. DOI: https://doi.org/10.1016/j.conbuildmat.2010.03.007.

[26] Y. De Santis, A. Aloisio, I. Gavrić, I. Sustersic, and M. Fragiacomo, "Timber-to-steel inclined screws connections with interlayers: Experimental investigation, analytical and finite element modelling," *Engineering Structures*, vol. 292, p. 116 504, Jun. 2023. DOI: 10.1016/j.engstruct.2023.116504.

[27] Deutsches Institut für Bautechnik, "ETA-11/0190," Deutsches Institut für Bautechnik, Berlin, Jul. 23, 2018. [Online]. Available: https://www.dibt.de/en/service/approval-download/detail/eta-110190.

[28] European Committee for Standardization, *EN 26891:1997 - timber structures - joints made with mechanical fasteners - general principles for the determination of strength and deformation characteristics*, Brussels, Belgium, 1997.

[29] RISE. "Digital image correlation measurement in mechanical testing." (May 2, 2023), [Online]. Available: https://www.ri.se/en/what-we-do/expertises/digital-image-correlation-measurement.

DEPARTMENT OF STRUCTURAL ENGINEERING
CHALMERS UNIVERSITY OF TECHNOLOGY
Gothenburg, Sweden
www.chalmers.se

CHALMERS